Natarajan Meghanathan
Jan Zizka (Eds)

Computer Science & Information Technology

3rd International Conference on Computer Science, Information Technology and Applications (CSITA - 2017)
October 28~29, 2017, Dubai, UAE

AIRCC Publishing Corporation

Volume Editors

Natarajan Meghanathan,
Jackson State University, USA
E-mail: nmeghanathan@jsums.edu

Jan Zizka,
Mendel University in Brno, Czech Republic
E-mail: zizka.jan@gmail.com

ISSN: 2231 - 5403
ISBN: 978-1-921987-73-1
DOI : 10.5121/csit.2017.71401 - 10.5121/csit.2017.71405

Typesetting: Camera-ready by author, data conversion by NnN Net Solutions Private Ltd., Chennai, India

Preface

The 3rd International Conference on Computer Science, Information Technology and Applications (CSITA - 2017) was held in Dubai, UAE, during October 28~29, 2017. The 3rd International Conference on Data Mining and Applications (DMAP - 2017), The 3rd International Conference on Image and Signal Processing (ISPR - 2017) and The 3rd International Conference on Networks, Mobile Communications (NMCO - 2017) was collocated with The 3rd International Conference on Computer Science, Information Technology and Applications (CSITA - 2017). The conferences attracted many local and international delegates, presenting a balanced mixture of intellect from the East and from the West.

The goal of this conference series is to bring together researchers and practitioners from academia and industry to focus on understanding computer science and information technology and to establish new collaborations in these areas. Authors are invited to contribute to the conference by submitting articles that illustrate research results, projects, survey work and industrial experiences describing significant advances in all areas of computer science and information technology.

The CSITA-2017, DMAP-2017, ISPR-2017, NMCO-2017 Committees rigorously invited submissions for many months from researchers, scientists, engineers, students and practitioners related to the relevant themes and tracks of the workshop. This effort guaranteed submissions from an unparalleled number of internationally recognized top-level researchers. All the submissions underwent a strenuous peer review process which comprised expert reviewers. These reviewers were selected from a talented pool of Technical Committee members and external reviewers on the basis of their expertise. The papers were then reviewed based on their contributions, technical content, originality and clarity. The entire process, which includes the submission, review and acceptance processes, was done electronically. All these efforts undertaken by the Organizing and Technical Committees led to an exciting, rich and a high quality technical conference program, which featured high-impact presentations for all attendees to enjoy, appreciate and expand their expertise in the latest developments in computer network and communications research.

In closing, CSITA-2017, DMAP-2017, ISPR-2017, NMCO-2017 brought together researchers, scientists, engineers, students and practitioners to exchange and share their experiences, new ideas and research results in all aspects of the main workshop themes and tracks, and to discuss the practical challenges encountered and the solutions adopted. The book is organized as a collection of papers from the CSITA-2017, DMAP-2017, ISPR-2017, NMCO-2017.

We would like to thank the General and Program Chairs, organization staff, the members of the Technical Program Committees and external reviewers for their excellent and tireless work. We sincerely wish that all attendees benefited scientifically from the conference and wish them every success in their research. It is the humble wish of the conference organizers that the professional dialogue among the researchers, scientists, engineers, students and educators continues beyond the event and that the friendships and collaborations forged will linger and prosper for many years to come.

Natarajan Meghanathan
Jan Zizka

Organization

General Chair

David C. Wyld	Southeastern Louisisna University, USA
Jan Zizka	Mendel University in Brno, Czech Republic

Program Committee Members

Ahmed Korichi	University of Ouargla, Algeria
Atallah M	AL-Shatnawi, Al al-Byte University, Jordan
Brajesh Kumar	Indian Space Research Organization, India
Christophe Claramunt	Naval Academy Research Institute France, France
Da Yan	The University of Alabama at Birmingham, USA
Dinesha Chathurani N	Queensland University of Technology, Australia
Dongchen Li	Peking University, China
Elaheh Pourabbas	National Research Council, Italy
Emad Awada	Applied Science University, Jordan
Eng. Wael abou el-wafa	Minia university, Egypt
Faiz ul haque Zeya	Bahria University, Pakistan
Fouzi Lezzar	Abdelhamid Mehri-Constantine 2 University, Algeria
Gelenbe	Imperial College, UK
Giuseppe Manco	ICAR-CNR, Italy
Goreti Marreiros	Polytechnic of Porto, Portugal
Hamid Alasadi	Basra University, Iraq
Hayet Mouss	Batna Univeristy, Algeria
Hu, Yu-Chen	Providence University, Taiwan
Isa Maleki	Islamic Azad University, Iran
Jamal El Abbadi	Mohammadia V University Rabat, Morocco
Jan Lindstrom	MariaDB Corporation, Finland
Jayan V	CDAC Trivandrum, India
Jose Antonio Correia	University of Porto, Portugal
Jose Maria Luna Ariza	Univerisity of Cordoba, Spain
Jose Raniery	University of Sao Paulo, Brazil
Juan Manuel Corchado Rodríguez	University of Salamanca, Spain
Jun Zhang	South China University of Technology, China
Jyrki Nummenmaa	University of Tampere, China
Leandro Carlos de Souza	Universidade Federal Rural do Semi-Árido, Brazil
Marcelo Ladeira	University of Brasilia, Brazil
Márcia	IBM Research Brazil, Brazil
Marco Anisetti	University of Milan, Itlay
Mario Henrique Souza Pardo	University of São Paulo, Brazil
Mastaneh Mokayef	UCSI University, Malaysia
Mehrdad Jalali	Mashhad Azad University, Iran
Meriem bensouyad	Université Mentouri de Constantine, Algeria
Metais Elisabeth	Le Cnam, France

Mohamedmaher Benismail	King Saud University, Saudi Arabia
Mohammad Rawashdeh	University of Central Missouri, United States
Mohammed AbouBakr Elashiri	Beni Suef University, Egypt
Mostafa Ashry	Alexandria University, Egypt
Noura Taleb	Badji Mokhtar University, Algeria
Pedro Henriques Abreu	University of Coimbra, Portugal
Rim Haddad	Innov'com Laboratory, Tunisia
Samad Kolahi	Unitec Institute of Technology, New Zealand
Samadhiya	National Chiao Tung University, Taiwan
Seyed Ziaeddin Alborzi	Universite de Lorraine, France
Soha Mohamed	Harbin institute of technology, Egypt
Tahmid Rahman Laskar	Leading University, Bangladesh
Tranos Zuva	Tshwane University of Technology, South Africa
Xiao Zhang	University of Denver , USA
Yue Guo	Hohai University, China

Technically Sponsored by

Computer Science & Information Technology Community (CSITC)

Networks & Communications Community (NCC)

Digital Signal & Image Processing Community (DSIPC)

Organized By

Academy & Industry Research Collaboration Center (AIRCC)

TABLE OF CONTENTS

3rd International Conference on Computer Science, Information Technology and Applications (CSITA - 2017)

3rd International Conference on Data Mining and Applications (DMAP - 2017)

3rd International Conference on Image and Signal Processing (ISPR - 2017)

3rd International Conference on Networks, Mobile Communications (NMCO - 2017)

REDUCING THE MONITORING REGISTER FOR THE DETECTION OF ANOMALIES IN SOFTWARE DEFINED NETWORKS

Luz Angela Aristizábal Q.[1] and Nicolás Toro G.[2]

[1]Department of Computation, Faculty of Management,
National University, Manizales, Colombia
[2]Department of Electrical and Electronic Engineering,
National University, Manizales, Colombia

ABSTRACT

Reducing the number of processed data, when the information flow is high, is essential in processes that require short response times, such as the detection of anomalies in data networks. This work applied the wavelet transform in the reduction of the size of the monitoring register of a software defined network. Its main contribution lies in obtaining a record that, although reduced, retains detailed information required by the detectors of anomalies.

KEYWORDS

Network Monitoring, anomalies Detectors, Software Defined Networking (SDN), Wavelet transform

1. INTRODUCTION

Monitoring the activity of a data network involves the verification of operating limits such as changes in bandwidth that ensure quality of service (QoS), congestion levels of servers and interconnection devices, safety conditions, etc. This verification is a constant activity that requires the analysis of large volumes of information and short response times, and it is an activity that must compensate the overhead in the measurement and its accuracy [1].

Traffic measurement approaches are active and passive. The passive methods take measurements from traffic passing through network devices without introducing overhead, whereas active methods add traffic to the network by sending packets that are used to obtain network parameters, for example, latency of a link or of some device. [2].

With the emergence of software-defined networks in 2008, a new prospect for the implementation of network monitors was visualized. In its operation model, each switch connected to a controller also includes the generation of statistics associated with the flows of data circulating through its ports. [3] [4] This makes the implementation of passive monitoring simpler, although with the difficulty involved in the analysis of large volumes of information [5]. Subsampling techniques have been used in passive monitoring in order to reduce the amount of data in analysis processes [6][8]. However, for an abnormalities detector to achieve a high accuracy, it is necessary to

Natarajan Meghanathan et al. (Eds) : CSITA, DMAP, ISPR, NMCO - 2017
pp. 01– 07, 2017. © CS & IT-CSCP 2017 DOI : 10.5121/csit.2017.71401

consider as many statistics as the network can provide, which can be achieved by considering all the statistical information that the switches of the software defined network can send to controller.

Our interest was considering the wavelet transform as a method that could reduce the statistics data number generated in the network, retaining the level of detail that a detector needs for the evaluation of anomalous behaviours.

The results were evaluated by considering the percentage of data reduction and contrasting the reliability of the anomalies detector with original and reduced data.

This article begins by illustrating the structure of software defined networks and the statistics obtained by network switches. It continues with the explanation of the transform wavelet and concludes with the experimental results.

2. SOFTWARE DEFINED NETWORK

2.1. Structure

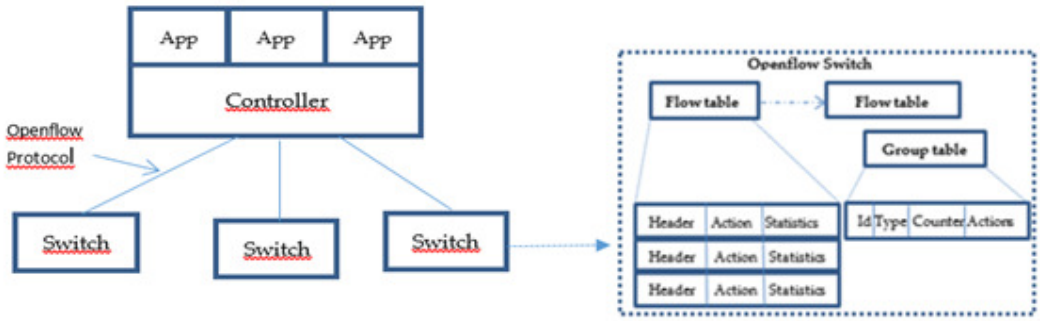

Figure 1. Software Defined Network

A Software-defined network (SDN) consists of at least two parts: controllers and interconnection devices, such as switches and routers, fig 1. The switches basically forward data according to the forwarding policies considered by the controller. A controller is a centralized software that tells the switch what to do with incoming data flows: It determines which port will forward the data and if it is necessary to duplicate or drop the data. This decision is made with each data flow that arrives to switch. The communication between switches and controllers is established by using the protocol "openflow" [4]. An Openflow switch has a flow table, each entry consists of header fields, which identify the incoming flow, an action on the flow and statistics information (right table in fig 1).

When a packet enters the switch, its fields are compared with the table header. If they match, the corresponding actions are realized.

Unlike traditional networks, the software-defined network allows: [3][9]

1. The controller to update the switch's flow table with rules on execution time
2. The controller to request the traffic statistics from switches.
3. The data path of flows to change at runtime

These characteristics make the data network more flexible, facilitating the implementation of strategies that make it safer and more dynamic.

2.2. Statistics Information.

Openflow switches send statistical information to the controller when required: Per interface, flow, queue and table.

We choose the interface statistics to illustrate the effectivity of the wavelet transform. The information that the openflow switch sends to the controller includes received packets, transmitted packets, received bytes, transmitted bytes, receive drops, transmitted drops, received errors, and transmitted errors.

The exchange of information between the openflow switch and controller is made with two messages: *Statistics Request* is used by the controller to request statistical information to the switch and *Statistics Reply* is sent by the switch to the controller in response to a request.

The algorithms implemented to obtain the statistics begin with a temporizer with an interval of 20 s. The controller sends a request message to all the connected switches each time the temporizer changes. After the controller receives the answer from the switches, it chooses the ports associated with the servers and it sends that information to the anomalies detector.

3. REDUCTION OF REGISTER

Based on the hypothesis that the performance register of a node on a data network under normal conditions presents little variation (low frequencies), and that a relatively abrupt or atypical change in the behavior of the node would result in the appearance of high frequencies, we chose to implement the wavelet transform that provides information about spatiality and frequency and that is proportional to the changes of the wavelet in the transform (The factor k in equation 1). Depending of this factor the wavelet ($\psi(t)$) shrinks or dilates [7]. When the analyzed register has low frequencies, a dilated wavelet will allow to obtained coefficients of high value, indicating the presence of low frequencies; when the register has high frequencies, a contracted wavelet would allow to obtain coefficients of high value, indicating the presence of high frequencies. The more similar the wavelet to the form of the network activity register, the wavelet coefficients will be higher in a given time [1]

$$W(d,k) = \int_{-\alpha}^{\alpha} x(t) \frac{1}{\sqrt{|k|}} \psi\left(\frac{t-d}{k}\right) dt \qquad (1)$$

Equation 1. Wavelet transform.

At the discrete level the transform is implemented using a bank of filters, the low pass filters perform the process similar to that performed in the continuous transformation when having a high scaling factor (low frequency extraction) and filters high pass have the same effect of calculating the transform with a small scale factor (high frequency extraction). Dado que nos interesa reducir el número de valores que conforman el registro se utilizó el método “wavelet packed”, ilustrado en la fig. 2.

The implementation consists in the application of a bank of filters one step low (LP) and another step high (HP), whose coefficients are determined by the base wavelet. In this case, the Register (i) is filtered by performing the convolution operation obtaining register (i + 1) with a larger

number of samples with respect to the signal of the upper level of the transformation tree, which makes it necessary to apply a subsampling reduces the number of samples in half, for each time the filters are applied. ***Thus in the third level of the tree we would have a signal of 256 samples, when the original signal initiated the process with 1024 samples***. The decision to continue applying the discrete transform is determined by the energy level of the filtered signal. If we take the fig. 3 the tree expands by the LP branch, which implies that the energy of the LP register (i + 1) signal is greater than the HP (i + 1).

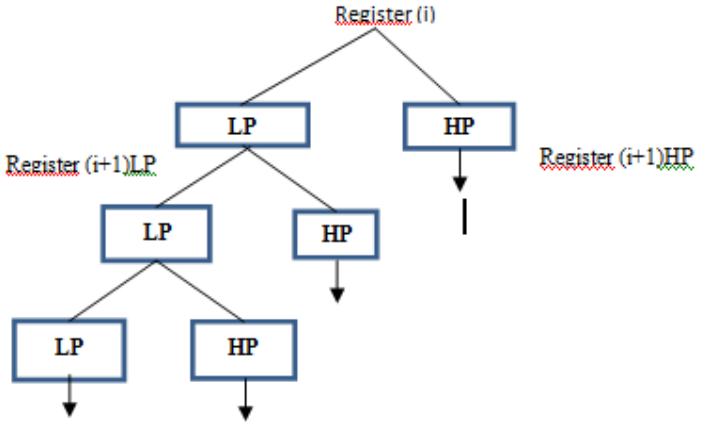

Figure 2. Descompositon tree. Discrete wavelet transform.

4. EXPERIMENTAL RESULTS

Since the basic objective of this work was to determine the reliability of the application of the wavelet transform in order to reduce the size of the statistical records obtained by the controller in a software-defined network, we considered the statistics of the associated interfaces with servers in a mininet simulation environment to reduce the sequence of transmitted bytes. (see fig 3).

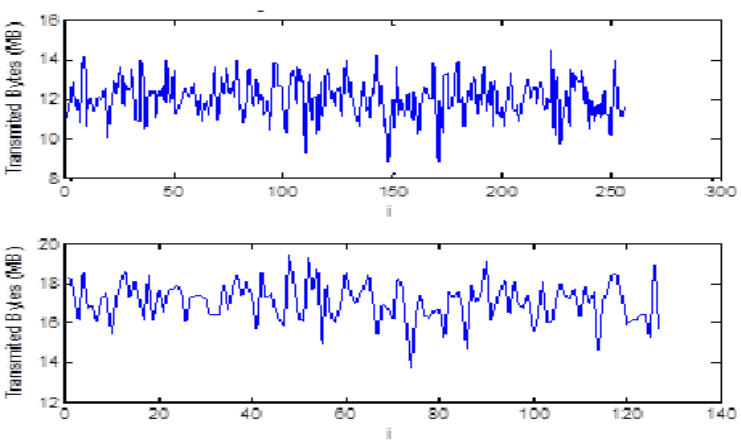

Figure 3. Reduction of register with wavelet transform

The upper graph represents the original register and shows 256 values of transmitted bytes. The lower graph represents the reduced register with 128 values, showing a good approximation to the waveform and a reduction of 50% of the original register.

We carried out the synthesis process to determine the effectiveness of the application of the wavelet transform for this type of data. We applied the inverse wavelet transform to the output of the filter banks. Fig. 4 shows the similarity between the two registers.

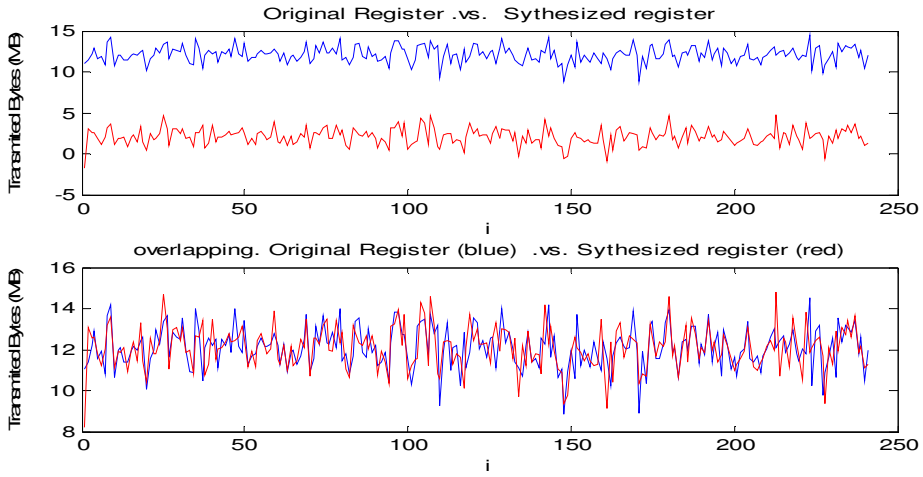

Figure 4. Comparison between the original register (blue) and the wavelet synthesized register (red).

We applied a Gaussian anomalies detector to the original and synthesized register to determine the effectiveness of the wavelet transform in the conservation of atypical data. See fig. 5. The atypical values are marked with red circles.

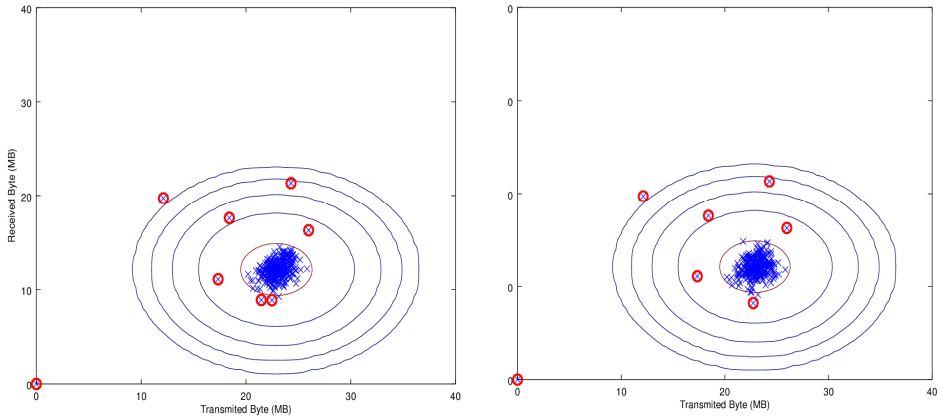

Figure 5. Result of anomaly detector. Left, Original data. Right synthetized register.

We concluded by observing how atypical behavior was conserved in fig. 6.

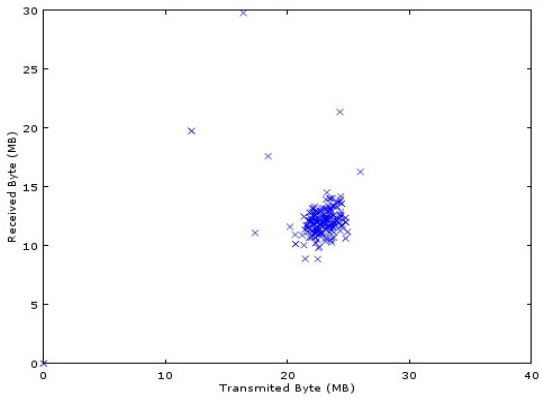

Figure 6. Relation of atypical points in the reduced register.

With this last result, we were able to verify that the detection of anomalies can be done with a shorter register than the original. This will generate less costs for computing processes and the storage of data.

5. CONCLUSIONS

The algorithm of reduction has a compression factor of at least a 50%. It *retains the atypical behaviour* of statistics data generated by the Openflow switch, which reduces the execution time of an anomaly detector.

The results of this work leave a door open for the analysis of the effectiveness of other wavelet bases in the reduction of the length of the statistical parameters in Software Defined Networks. Since this work only used the "daubechies" wavelet, evaluating other base wavelets could lead to a better reduction rate.

REFERENCES

[1] Ibidunmoye, Olumuyiwa, Hernandez R Francisco, Elmroth Erick .(2015) “Performance Anomaly Detection and Bottleneck Identification”. ACM Computing Surveys, Vol. 48, No. 1, Article 4.

[2] M, Jammal, T. Singh, A. Shami, R.l Asal, Y. Li, (2014) "Software defined networking: State of the art and research challenges", Computer Networks.

[3] Dabbagh, B.Hamdaoui, M. Guizani, and A. Rayes,(2015) "Software-Defined Networking Security: Pros and Cons", IEEE Communications Magazine.

[4] N, S. Bailey, Deepak Bansal, Linda Dunbar, Dave Hood, Zoltán Lajos Kis, (2012) "SDN Architecture Overview”. Open Network Foundation. (https://www.opennetworking.org/images/stories/downloads/sdnresources/technical-reports/SDN-architecture-overview-1.0.pdf)

[5] K. Giotis, C. Argyropoulos, G. Androulidakis, D. Kalogeras, V. Maglaris, (2014) "Combining OpenFlow and sFlow for an effective and scalable anomaly detection and mitigation mechanism on SDN environments”, Computer pag. 122–136

[6] L. Jose, M. Yu, and J. Rexford, (2011) “Online measurement of large traffic aggregates on commodity switches”, in Proc. of the USENIX workshop.

[7] Stéphane. Mallat, (2008) “A wavelet tour of signal processing”. Academic Press, USA.

[8] L. Kalinichemko, I. Shanin, I. Taraban,(2014) "Methods for Anormaly Detection: a Survey", Advanced Methodos and Technologies, digital collections. Pag. 20-25.

[9] M. Dabagh, B. Handaoul, M. Guizani, A. Rayes, (2015) "Software-Defined Networking Security: Pro and Cons", IEEE Communications Magazine. pags. 73-79.

[10] L. Seunghyeon, K. Jinwoo, S. Seungwon, P. Porras, (2017). "Athena: A framework for scalable Anormaly Detection in Software Defined Networks",47th Annual IEEE/IFIP International Conference on Dependable Systems and Networks. Pags 249-260.

AUTHORS

Luz A. Aristizábal Q. is a professor in the Department of Computing in the Faculty of Management at the National University of Colombia. She received her MEng in Physical Instrumentation from the Technological University of Pereira in 2009, her degree in Data Networks Specialization from Valle University in 1991, and her degree in Engineering Systems from Autónoma University in 1989. Her research focuses on aspects of computer and data networks, including the network simulators, signal processing and network paradigms.

Nicolás Toro G. is a professor in the Department of Electrics, Electronics and Computing. He received his PhD in Engineering-Automation and SB in Electrical Engineering from the National University of Colombia in 2013 and 1983 respectively, and his MEng degrees in Automated production systems from the Technological University of Pereira in 1992. His research focuses on many aspects of industrial automation, including the design, measurement, and analysis of networks.

INTENTIONAL BLANK

IMPROVE THE QUALITY OF IMPORTANT SENTENCES FOR AUTOMATIC TEXT SUMMARIZATION

Michael George

Department of Information Technology, Dubai Municipality, Dubai City, UAE

ABSTRACT

There are sixteen known methods for automatic text summarization. In our study we will use Natural language processing NLP within hybrid approach that will improve the quality of important sentences selection by thickening sentence score along with reducing the number of long sentences that would be included in the final summarization. The based approach which is used in the algorithm is Term Occurrences.

KEYWORDS

Text summarization, Data mining, Natural language processing, Sentence scoring, Term Occurrences.

1. AIM

This research will provide an algorithm to improve important sentences quality for automatic text summarization. This method suitable for search engines, business intelligence mining tools, single document summarization and filtered summarization that rely on the top short list of important sentences.

2. INTRODUCTION

Automatic Text summarization [1] is a mechanism of generating a short meaningful text that can summarize a textual content by using computer algorithm. The quality of the summarization depends on the quality of the selection ability of the important sentences, paragraphs out of the main document that was given as input. That list of the sentences will be used in the formation of the final summarization with different custom ways which will represent the original content.

Automatic Text summarization is sub method in Data mining. And it is necessary in many sectors such as Search engines, Education, Business intelligence, Social media, and e-commerce.

As one of artificial intelligence functions, automatic text summarization have sensitive operations that require accuracy for meanings capturing, since there is no awareness to understand the

Natarajan Meghanathan et al. (Eds) : CSITA, DMAP, ISPR, NMCO - 2017
pp. 09– 15, 2017. © CS & IT-CSCP 2017 DOI : 10.5121/csit.2017.71402

content. Recently as data became large enough that makes easy classification is big challenge, while natural language processing NLP [2] tools advancing and as it's the backbone for text summarization, approaches and algorithms been developed to reform and improve the quality of the output. It become necessary to shorthand the data with the most important content text summarization is an efficient method for knowledge mining and extraction for many different sector.

Text Summarization Methods and approaches which currently in Development such as Neural networks [5], Graph theoretic [6], Term Frequency-Inverse Document Frequency (TF IDF) [7][8], Cluster based [8], Machine Learning [9], Concept Oriented [10], fuzzy logic [11][12][13], Multi document Summarization[14][15], Multilingual Extractive [16][17].

We are addressing the techniques that improves term occurrence processing that gives better score for the sentences selected to be included in the summarization.

3. RELATED WORK

3.1. Term Frequency-Inverse Document Frequency (TF IDF) approach

TF IDF stands for term frequency-inverse document frequency, and the tf-idf [7][8][3] weight is a weight often used in information retrieval and text mining. This weight is a statistical measure used to evaluate how important a word is to a document in a collection or corpus. The importance increases proportionally to the number of times a word appears in the document but is offset by the frequency of the word in the corpus. Variations of the tf-idf weighting scheme are often used by search engines as a central tool in scoring and ranking a document's relevance given a user query.

TF: Term Frequency, which measures how frequently a term occurs in a document. Since every document is different in length, it is possible that a term would appear much more times in long documents than shorter ones. Thus, the term frequency is often divided by the document length, the normalization equation:

$$\mathrm{tf}_{i,j} = \frac{n_{i,j}}{\sum_k n_{k,j}}$$

Where ni,j is the number of occurrences of the considered term (ti) in document dj, divided by ∑k nk, j which is the total number of words in document dj.

IDF: Inverse Document Frequency is a measure of how much information the word provides, that is, whether the term is common or rare across all documents. It is the logarithmically scaled inverse fraction of the documents that contain the word, obtained by dividing the total number of documents by the number of documents containing the term, and then taking the logarithm of that quotient as the following equation:

$$\mathrm{idf}_i = log \frac{|D|}{1 + |\{j : t_i \in d_j\}|}$$

Where |D| : total number of documents in the corpus divided by {j: ti ∈ dj}: number of documents where the term t appears, if the term is not in the corpus, this will lead to a division by zero. It is therefore common to adjust the denominator to 1 + {j: ti ∈dj} and in that cases which the inputs is a single document only, then IDF value will = 1.

Then we have the value of TF-IDF as TF * IDF for each term.

By sorting the results descending, we will get the highest terms in the given inputs.

3.2. Important sentences using Term Frequency

Usually the evaluation of sentence score, equal the sum of total terms value in the sentence, first split the document into sentences and counting the score for each sentence then sort them down descending to get the top sentences which would include in the summarization. Terms denseness gives the sentence its score.

4. THE METHODOLOGY AND ALGORITHM

We developed an approach we called it thick sentences that thickening sentence score which is Re-filtering important sentences, to fetch sentences with higher value and density and lower length. In short it's summarizing the summarization.

Our target is increasing sentence value along with reducing unnecessary words and long sentences, which make the top sentences list has more value. So that sentence score equal total sentence terms occurrence divided by sentence words, as the following equation:

$$SS = \frac{\sum TOC}{SW_n}$$

Where SS is the total sentence score and ∈ TOC (term occurrence count) is sum of sentence terms occurrence (number of appearance in the whole document\s), SWn is the sentence words count.

4.1. Data Extraction and procedure steps

- **Sentences splitting**: split the inputs (document/s) into array of sentences to improve terms fetching.

- **Natural Language Processing NLP**: in this part we used NLP Tools [4] to extract the keywords from the each sentence which have meaningful value such as nouns and adjectives, excluding stop words which can give false result. In term frequency approach, terms extraction happens once and globally for the entire inputs and getting high terms by filtering the top terms based on their frequency. In our method terms extraction happens for each sentence separately to reduce the time for terms comparison and avoiding missing terms.

- **Loop and indexing**: each sentence had index with the array of terms related, indexing the sentence to define its score based on evaluation result.

- **Score Evaluation**: applying our method on each sentence loop to get each score from related terms, as per the formula "SS = ∈TOC / SWn".

- **Promote important sentences**: sort the results based on score descending and get top sentences.

4.2. Algorithm

```
_____________________________________________________
N = the number of all sentences in the entire input
FOR  i = 0 To N
      SS = 0 'sentence score'
      TOC = 0 'terms Occurrence'
      ST = List of terms for (N -i)

      FOR  j = 0 To ST
         TOC = TOC + (ST-j n) 'term Occurrence'
      END LOOP

      SS = TOC / (N -i)Wn

      IF SS > 0 THEN
         AddToImportantSentencesList(N-i 'Current Sentence', SS)
END LOOP
_____________________________________________________
```

Algorithm Output was the list of important sentences sorted descending by score. The method shows good results if the target was fetching a short number of top sentences.

5. RESULTS

We tested our method on Science-space articles from (20 newsgroups datasets) [18], in the following table the results of top ten sentences in comparison with the initial term frequency method, sorted by our score descending.

As the both approaches are dealing with terms occurrence to promote the important sentences, the advantage here that we reduced results length, without losing the value of meaning or terms.

As we can see in "Table 1" we are getting short sentence in the top along with high terms occurrence by sorting by our score.

Where the sentences are contain strong related terms in most of its words.

Table 1. Score comparison for 20 newsgroups dataset.

Sentence.	Words Count.	TF Score	Our Score.
1st	11	1.06	7.91
2nd	6	0.55	7.83
3rd	30	2.83	7.73
4th	9	0.82	7.67
5th	12	1.08	7.58
6th	21	1.90	7.52
7th	9	0.82	7.44
8th	38	2.91	5.95
9th	16	1.20	5.88
10th	25	1.80	5.88

6. CONCLUSIONS

Clean selection of important sentences is the first stage to have efficient summarization. Sentence score is in making by many approaches, term frequency is one of the best methods from important sentences detection. By using thick sentences we have better quality as we can see from the following points.

- Promote short sentences which has a high terms occurrence.
- Unload unnecessary words which can increase the final summarization.
- Fast implementation from logic side.
- Summarize the summarization.

In this study we reviewed the main methods and ways to summarize text, we improved the term occurrence method by thickening sentence score and our system used C# 4.0 framework and Apache OpenNLP [4].

7. FUTURE WORK

Our equation was developed for specific scope that will be used mostly for web content.

The challenge when we tested the same approach but with larger inputs which contains a huge number of documents such as large books, then the results had less quality as term occurrence will not give accurate values and therefore the equation need to be adapted to cover this gap.

8. SUPPLEMENTARY MATERIAL

As it is about text summarization, so we used our method to summarize our paper itself and include top 5 sentences here as secondary visual result in the following Table.

Table 2. top 5 important sentences in the current paper

Sentence	Score
automatic text summarization is sub method in data mining	6.33
terms denseness gives the sentence its score	5.71
promote important sentences: sort the results based on score descending and get top sentences	5.33
this research will provide an algorithm that improves important sentences quality for automatic text summarization	4.88
sentence score is in making by many approaches, term frequency is one of the best methods from important sentences detection	4.5
this method suitable for search engines, business intelligence mining tools, single document summarization and filtered summarization that rely on the top short list of important sentences	4.31

ACKNOWLEDGEMENTS

I would like to Thank all those who Supported and encourage me, and for whom helped on that research, also thanks to Dubai Municipality for the good environment, tools and support from great management.

REFERENCES

[1] Aarti Patil, Komal Pharande, Dipali Nale, Roshani Agrawal "Automatic Text Summarization" Volume 109 – No. 17, January 2015.

[2] Ronan Collobert, “Natural Language Processing (Almost) from Scratch” 2011.

[3] TF-IDF "term frequency-inverse document frequency" tfidf.com.

[4] NLP "Apache OpenNLP" opennlp.apache.org.

[5] Khosrow Kaikhah, "Automatic Text Summarization with Neural Networks", in Proceedings of second international Conference on intelligent systems, IEEE, 40-44, Texas, USA, June 2004.

[6] G Erkan and Dragomir R. Radev, “LexRank: Graph-based Centrality as Salience in Text Summarization”, Journal of Artificial Intelligence Research, Re-search, Vol. 22, pp. 457-479 2004.

[7] Joeran Beel "Research-paper recommender systems: a literature survey" November 2016, Volume 17, Issue 4, pp 305–338.

[8] KyoJoong Oh "Research Trend Analysis using Word Similarities and Clusters" Vol. 8, No. 1, January, 2013.

[9] Joel larocca Neto, Alex A. Freitas and Celso A.A.Kaestner, "Automatic Text Summarization using a Machine Learning Approach”, Book: Advances in Artificial Intelligence: Lecture Notes in computer science, Springer Berlin / Heidelberg, Vol 2507/2002, 205-215, 2002.

[10] Meng Wang, Xiaorong Wang and Chao Xu, "An Approach to Concept Oriented Text Summarization", in Proceedings of ISCIT’05, IEEE international conference, China,1290-1293, 2005.

[11] Farshad Kyoomarsi, Hamid Khosravi, Esfandiar Eslami and Pooya Khosravyan Dehkordy, "Optimizing Text Summarization Based on Fuzzy Logic", In proceedings of Seventh IEEE/ACIS International Conference on Computer and Information Science, IEEE, University of Shahid Bahonar Kerman, UK, 347-352, 2008.

[12] Ladda Suanmali, Mohammed Salem, Binwahlan and Naomie Salim, "Sentence Features Fusion for Text summarization using Fuzzy Logic, IEEE, 142-145, 2009.

[13] Ladda Suanmali, Naomie Salim and Mohammed Salem Binwahlan, "Fuzzy Logic Based Method for Improving Text Summarization", (IJCSIS) International Journal of Computer Science and Information Security, Vol. 2, No. 1, 2009.

[14] Junlin Zhanq, Le Sun and Quan Zhou, "A Cue-based HubAuthority Approach for Multi-Document Text Summarization", in Proceeding of NLP-KE'05, IEEE,642- 645, 2005.

[15] Chin-Yew Lin and Eduard Hovy," From Single to Multidocument Summarization: A Prototype System and its Evaluation", Proceedings of the ACL conference, pp. 457–464. Philadelphia, PA. 2002.

[16] David B. Bracewell, Fuji REN and Shingo Kuriowa, "Multilingual Single Document Keyword Extraction for Information Retrieval", Proceedings of NLP-KE'05, IEEE, Tokushima, 2005.

[17] Dragomir Radev "MEAD - a platform for multi document multilingual text summarization", In Proceedings of LREC 2004, Lisbon, Portugal, May 2004.

[18] 20 newsgroups, "Naive Bayes algorithm for learning to classify text" cs.cmu.edu.

AUTHOR

Michael George Girgis, born in Cairo Egypt, 1987,
A Software engineer, specialist in Data mining and machine learning algorithms
Has a Bachelor degree in Management Information systems,
From Obour Academy Cairo, Egypt.
Interested in Addressing Association and text Analysis Algorithms.

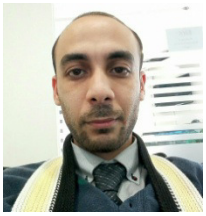

INTENTIONAL BLANK

A NOVEL METHOD FOR WATERLINE EXTRACTION FROM REMOTE SENSING IMAGE BASED ON QUAD-TREE AND MULTIPLE ACTIVE CONTOUR MODEL

Zhang Baoming, Guo Haitao, Lu Jun and Yu Jintao

Zhengzhou Institute of Surveying and Mapping, Zhengzhou 450052, China

ABSTRACT

After the characteristics of geodesic active contour model (GAC), Chan-Vese model (CV) and local binary fitting model (LBF) are analyzed, and the active contour model based on regions and edges is combined with image segmentation method based on quad-tree, a waterline extraction method based on quad-tree and multiple active contour model is proposed in this paper. Firstly , the method provides an initial contour according to quad-tree segmentation; secondly, a new signed pressure force (SPF) function based on global image statistics information of CV model and local image statistics information of LBF model has been defined, and then, the edge stopping function(ESF) is replaced by the proposed SPF function, which solves the problem such as evolution stopped in advance and excessive evolution; finally, the Selective Binary and Gaussian Filtering Level Set method is used to avoid reinitializing and regularization to improve the evolution efficiency. The experimental results show that this method can effectively extract the weak edges and serious concave edges, and owns some properties such as sub-pixel accuracy, high efficiency and reliability for waterline extraction.

KEYWORDS

Quad-tree; GAC model; CV model; LBF model; Waterline extraction

1. INTRODUCTION

The waterline extraction for coastal zone and island (reef) image is the basis to obtain the marine-oriented geographical information by remote-sensing image, and the waterline thematic map got through this way is the key data [1-2] for analyzing the coastal evolution and the integrated coastal management. The waterline extraction is the key technology for coastline extraction [3-4], and it is with significant importance to detect and extract the navigation landmarks and navigation targets on remote-sensing image. Currently, there are various methods to extract the waterline from remote-sensing images. The most commonly used extraction methods include thresholding segmentation [5], edge detection method [2], active contour model method [6-8], level-set method [1], region growing method [9], etc. The thresholding segmentation method is simple to accomplish, with faster processing rate, but it is only suitable for segmenting the image with sharp contrast between the waters and the background. The position of the waterline extracted by

Natarajan Meghanathan et al. (Eds) : CSITA, DMAP, ISPR, NMCO - 2017
pp. 17– 34, 2017. © CS & IT-CSCP 2017 DOI : 10.5121/csit.2017.71403

the edge detection method is accurate, but the edge detected often contain disconnections, where subsequent edge processing is required; the level-set method is featured with strong anti-noise capacity, and the adaptivity of the curve topological changes is better, but with complicated algorithm, and its detection speed is relatively slow; the region growing method is capable to obtain intact waterline, but with unsatisfactory anti-noise performance, and the sudden change in the gray level of individual pixel near the seed pixel is prone to result in the skewing of the waterline easily[10]. The existing waterline extraction methods have three shortcomings [7] [11-12]: firstly, the extraction of weak edge waterline without obvious changes in gray level is not accurate; secondly, it is not easy to extract the waterline with complicated boundary accurately, especially the waterline with serious concave; thirdly, the seed region is required to be selected manually, with low automation and low efficiency. Therefore, it is hard to meet the requirements of follow-up study and automatic mapping.

The essence of waterline extraction is the segmentation of ocean-continent image. In recent years, the active contour model has been widely used in image segmentation [8-12]. This approach can be divided into boundary-based model and region-based model according to different driving force. Usually, the boundary-based active contour model utilizes the image gradient to construct the edge stopping function, thus ensuring to stop evolution at the contour of the target boundary; however, as this method utilizes the gradient information, it is hard for the evolution to stop at the target contour for the weak edge without obvious gradient changes [13], and the geodesic active contour(GAC) model is a typical boundary-based active contour model[10]. In terms of the region-based active contour model, the driving force of the contour model is based on the region statistical information of the image for construction; therefore, it is featured with better efficiency in segmentation of weak edge targets without obvious gradient or discrete boundary targets[13], and Chan-Vese (CV) model [12] is a typical region-based active contour model, and it is not sensitive to the initialization of the contour, but it cannot process the images with uneven gray level. Therefore, Li et al. proposed the regional variable active contour (LBF) model [14-15], which overcomes the shortcomings of CV model that it cannot segment the images with uneven gray level, but it is required to make convolution calculations, with large calculated amount, and it is more sensitive to the initialization of the contour. On such basis, the domestic and foreign scholars began to integrate the gradient information and the region information [16], integrate the local statistics and the global statistics [17], complement each other's advantages, and obtained better segmentation efficiency. The level-set method is the waterline extraction method for remote-sensing images of the coastal zone that has been studied more in recent years [1][6-8], especially the geometric active contour model method that integrates the level-set method and the active contour model, which is ideal for the waterline extraction by remote-sensing image. Literature [6] proposed an automatic ocean-land image segmentation method integrating the quad-tree and geometric active contour model, realizing the automatic rapid segmentation of the ocean-land image, but the segmentation effectiveness of the weak edge is not satisfactory; Literature [7] proposed a waterline extraction method based on Canny edge detection and GAC model, which has a better extraction efficiency for weak edge, and it is capable to extract the waterline with serious concave; however, the seed region is required to be selected manually, with low automation and long segmentation time. Literature [8] proposed an ocean-land image segmentation method integrating the quad-tree and the geodesic active contour model, which not only realizes the automatic rapid extraction, but also can extract the weak edge and the waterline with serious concave edges accurately, and by now, it is a method with better waterline extraction effectiveness that has been published newly.

Based on the analysis on the above methods, on the basis of analysis and study on GAC, CV and LBF model, this paper proposes a waterline extraction algorithm based on quad-tree and multiple active contour models, which can extract the weak edges and the waterlines with serious concave edges, with faster extraction speed and better stability.

2. WATERLINE EXTRACTION PRINCIPLE BASED ON QUAD-TREE AND MULTIPLE ACTIVE CONTOUR MODELS

2.1. Ocean-land image segmentation based on Quad-tree

In terms of the ocean-land remote-sensing image, the pixel gray value of its ocean part has a certain homogeneity and better connectivity, but on the whole, the grayscale is distributed unevenly, and the image edge has rich features as a whole relative to the sea area, especially the ocean-land boundary. According to this feature, the gradient is relatively small at the sea, while the gradient at the ocean-land boundary is relatively large; therefore, in order to facilitate the subsequent segmentation, the image gradient drawing shall be constructed first in accordance with Formula(1) [6]

$$G_{i,j} = \left[(g_{i,j} - g_{i+1,j})^2 + (g_{i,j} - g_{i,j+1})^2 \right]^{\frac{1}{2}} \tag{1}$$

The essence of the quad-tree segmentation is the integration of the regional divisions and the consolidation technology with the structure of the quad-tree, thus segmenting the image. The segmentation principle is as shown in Figure 1[6], and its advantage lies in the faster segmentation speed, and it is an automatic segmentation; however, it is unable to extract the weak edges and the serious concave edges accurately.

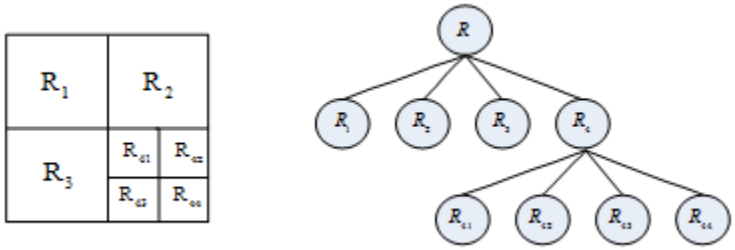

(a) Distinguished Images (b) Corresponding Quad-tree Structure

Fig.1 Structure Diagram for Quad-tree Segmentation

2.2. CV Model, LBF Model and GAC Model

(1) CV Model

The energy function of the CV model is [12]

$$E^{CV} = \lambda_1 \int_{inside(C)} |I(x,y) - c_1|^2 \, dxdy + \lambda_2 \int_{outside(C)} |I(x,y) - c_2|^2 \, dxdy \tag{2}$$

Whereas, $I(x, y)$ indicates the original image, and λ_1 and λ_2 are constants with positive value, in general, their value can be taken as $\lambda_1 = \lambda_2 = 1$. c_1 and c_2 indicate the mean value of the image grayscale inside and outside the contour curve respectively, with the calculation formula as follows:

$$\begin{cases} c_1(\phi) = \dfrac{\int_{\Omega} I(x, y) H_\varepsilon(\phi(x, y)) dxdy}{\int_{\Omega} H_\varepsilon(\phi(x, y)) dxdy} \\ c_2(\phi) = \dfrac{\int_{\Omega} I(x, y)(1 - H_\varepsilon(\phi(x, y))) dxdy}{\int_{\Omega} (1 - H_\varepsilon(\phi(x, y))) dxdy} \end{cases} \tag{3}$$

Whereas, the $H_\varepsilon(\phi(x, y)$ is the regularization of the Heaviside function, with its calculation formula as Formula (5), and $\phi(x, y)$ is the level set function.

In order to avoid the small and isolated areas as well as zero level set in the segmentation results in the end, this paper introduces the length penalty term and area penalty term, and obtains the evolution equation of the level set as follows:

$$\frac{\partial \phi}{\partial t} = \delta(\phi)[\mu \nabla(\frac{\nabla \phi}{|\nabla \phi|}) - \nu - \lambda_1 | I(x, y) - c_1 |^2 + \lambda_2 | I(x, y) - c_2 |^2] \tag{4}$$

Whereas, μ is a constant greater than 0, ν is usually taken as 0, ∇ is the gradient operator, $\delta(\phi(x, y))$ is the regularization of Dirac function, with the calculation formula as shown in Formula (5)

$$\begin{cases} H_\varepsilon(z) = \dfrac{1}{2}(1 + \dfrac{2}{\pi} \arctan(\dfrac{z}{\varepsilon})) \\ \delta(z) = \dfrac{1}{\pi} \cdot \dfrac{\varepsilon}{\varepsilon^2 + z^2}, z \in R \end{cases} \tag{5}$$

The CV model is a region-based active contour model, can detect weak edge target without obvious gradient changes [10]. Meanwhile, the CV model takes advantage of the global information of image; therefore, it is not sensitive to the initialization of contour, and is capable of processing the images with noise effectively. However, as this model considers the image as two constant regions, it is unable to process the image with uneven grayscale.

(2) LBF Model

The energy function of the CV model is

$$E^{LBF} = \lambda_1 \int_{\Omega} \int_{inside(C)} K_\sigma(x-y) \mid I(y) - f_1(x) \mid^2 dydx + \lambda_2 \int_{\Omega} \int_{outside(C)} K_\sigma(x-y) \mid I(y) - f_2(x) \mid^2 dydx \quad (6)$$

$$x, y \in \Omega$$

Whereas, the $I : \Omega \to R$ refers to the input image; λ_1 and λ_2 are constants with positive values, and the K_σ is the Gaussian kernel function with standard deviation of σ, f_1 and f_2 refer to the grayscale function of the local region inside and outside the image of the fitting contour respectively, with its formula as follows:

$$\begin{cases} f_1(x) = \dfrac{K_\sigma(x) * [H(\phi) I(x)]}{K_\sigma(x) * H(\phi)} \\ f_2(x) = \dfrac{K_\sigma(x) * [(1 - H(\phi)) I(x)]}{K_\sigma(x) * (1 - H(\phi))} \end{cases} \quad (7)$$

In order to maintain the stability and smoothness of the evolution, usually the length and signed distance constraints are introduced for level set evolution. The LBF model utilizes the local information, thus it does not have better segmentation efficiency for the images with uneven graysale; but with only local information, without global information involved, it is sensitive to the initial contour, and is featured with unsatisfactory anti-noise performance; what's more, it involves a great deal of calculation, thus limiting its application in practice.

(3) GAC Model

The principle of the GAC model is to minimize the following energy function

$$E^{GAC}(C) = \int_0^1 g(\mid \nabla IC(q) \mid) \mid C'(q) \mid dq \quad (8)$$

Whereas, $C(q)$ is the parameterized curve, and g is the edge stopping function.

Usually, in order to increase the evolution speed of the contour method on direction, a constant term α is added, adopting the minimum level set idea of Formula (8), and then the evolution equation of the level set is obtained as follows:

$$\frac{\partial \phi}{\partial t} = g \mid \nabla \phi \mid (div(\frac{\nabla \phi}{\mid \nabla \phi \mid}) + \alpha) + \nabla g \cdot \nabla \phi \quad (9)$$

Whereas, *div* refers to the divergent operator.

The GAC model relies on the edge gradient information to evaluate the curve, and is capable of processing the topology changes adaptively, provides high-precision closed segmentation curve, but it is sensitive to noise, so it is required to give initial contour manually, and is prone to get local minimum value and stops evolution for serious concave edge, thus affecting the extraction accuracy and reliability [16], as shown in Figure 2

(a) Initial Curve (b) Results of Evolution Reaching Steady State

Fig.2 Local Minimum Value Problem of GAC Model

When α is small, the segmentation curve stops evolution in advance before reaching the concave edge; but when α is too large, the possibility that the contour gets across the sharp edge increases; therefore, it is unable to extract the weak edges and the serious concave edges at the same time.

2.3. Waterline Extraction Based on Quad-tree and Multiple Active Contour Models

The above-mentioned models have their own advantages and disadvantages, and how to combine them mutually, to make up each other's deficiencies and to complete the segmentation of the images jointly are the hot points and difficult points of study in recent years. Literature [16] utilizes the CV model to improve the signed pressure force function and replaces the edge stopping function of GAC model, and such improvement highlights the segmentation target, and could improve the segmentation problems of weak edges and targets with uneven grayscale, and has the capacity of evolving the curve in dual direction: when the evolution curve is within the target, the curve evolves externally; when the evolution curve is outside the target, the curve evolves internally, thus reaching the target boundary finally. The influence of the signed pressure force function on curve evolution is as shown in Figure 3. The evolution equation of the level set is as shown in Formula (10)

(a) Original figure (b) Evolution curve outside the target (c) Evolution curve inside the target (d) Evolution curve goes across the target boundary

Fig.3 The Influence of Signed Pressure Force Function on Curve Evolution

$$\frac{\partial \phi}{\partial t} = spf\ (I) \cdot (div(\frac{\nabla \phi}{|\nabla \phi|}) + \alpha) |\nabla \phi| + \nabla spf\ (I) \cdot \nabla \phi \qquad (10)$$

Whereas, $spf\ (I)$ refers to the signed pressure force function.

Su Rina et al.[18] made use of the local region statistics of LBF model to improve the signed pressure force function, and proposed a new region-based active contour model. In view that CV model is unable to segment the images with uneven gray scale, while LBF model has a better effectiveness for such images. Therefore, this paper integrates the advantages of CV and LBF model to construct a new signed pressure force function

$$spf\ (I) = \frac{w \cdot (I - \frac{f_1 + f_2}{2}) + (1-w) \cdot (I - \frac{c_1 + c_2}{2})}{\max(w \cdot (I - \frac{c_1 + c_2}{2}) + (1-w) \cdot (I - \frac{f_1 + f_2}{2}))} \tag{11}$$

Whereas in Formula (11), $w(0 \le w \le 1)$ is a weight factor, and it can make adjustment according to the details of the image and the nonuniformity of the gray scale as determined by experience. In case of many image details or uneven gray scale, the value of w shall be small enough, which can be set as 0.1; otherwise, it shall be set as larger value, usually it can be set as w0.7, and then it could extract the edge better. The improved signed pressure force function can highlight the segmentation targets, and it has the capacity of dual-way evolution, thus improving the problem of GAC model effectively that it cannot extract the weak edges and serious concave edges at the same time. Therefore, the signed pressure force function constructed by this method can not only maintain the advantages of global information, and avoid the minimum evolution contour locally at the mean time during the level set evolution, but also maintain the advantages of local information, so it has a better effectiveness in the segmentation of image with uneven gray scale [16].

In Formula (11), $div(\nabla\phi/|\nabla\phi|)|\nabla\phi|$ is a regularization item, whose role is to regularize the level set function ϕ. As the level set function is a signed distance function and meets the requirement of $|\nabla\phi|=1$, then such regularization item meets the condition of $div(\nabla\phi/|\nabla\phi|)|\nabla\phi|=\Delta\phi$ [19], indicating that the regularization item can be expressed by the Laplace of the level set function ϕ. According to Literature [20] and the scale-space theory, if an evolution function evolves according to Laplace's equation, its effectiveness equates to the smoothing of gaussian kernel function for its initial contour. Therefore, the Gaussian filter can be used to replace this regularization item during the realization, and the $div(\nabla\phi/|\nabla\phi|)|\nabla\phi|$ in Formula (10) can be omitted. The re-initialization of the level set evolution has always been a difficulty for level set method, and in order to ensure the accuracy of the contour evolution, the re-initialization is applied in level set method [10], but there are errors between the theoretical and practical numerical implementation, so the re-initialization may make the zero level set deviate from its original position, and it involves a great deal of calculations, with low efficiency. In addition, it is hard to decide when and how to make initialization. Literature [17] proposed the Selective Binary and Gaussian Filtering Level Set (SBGFRLS) method is used to avoid reinitialization [21], and saves the reinitialization time, thus improving the evolution efficiency significantly. As the method adopted by this paper utilizes the region statistical information with broader boundary capture range, so the $spf\ (I)|\nabla\phi|$ in Formula (10) can also be omitted, and finally, the evolution equation is shown as follows:

$$\frac{\partial\phi}{\partial t} = spf\ (I) \cdot \alpha |\nabla\phi| \tag{12}$$

It can be seen from the above analysis that, the image segmentation algorithm based on quad-tree is featured with rapid segmentation speed and high level of automation, but it cannot segment the weak edges and serious concave edges accurately; therefore, this paper adopts the thoughts segmenting the given initial contour with quad-tree roughly at first, and then utilizing the multiple

active contour models for fine segmentation so as to get accurate results. This method can not only extract general waterline accurately, but also can extract the weak edges and the waterlines with serious concave edges.

The algorithm flow for waterline extraction based on quad-tree and multiple active contour models is as shown in Figure 4.

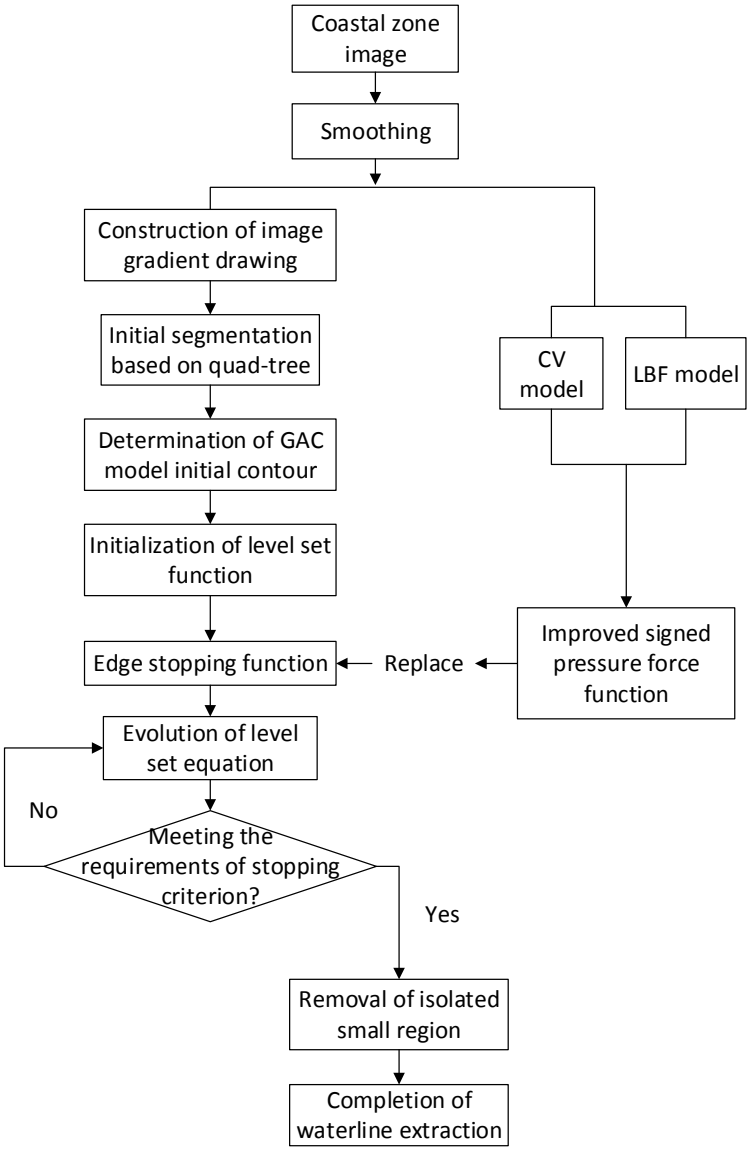

Fig.4 Flowchart for waterline extraction

3. EXPERIMENTAL FINDINGS AND ANALYSIS

In order to verify the effectiveness of the algorithm proposed by this paper, multiple groups of experiments were conducted, and analysis was also made to compare with other 3 waterline extraction methods. In order to analyze the extraction efficiency of these four methods quantitatively, 6 groups of experiments were listed below, which made statistics and verification from four aspects, including extraction precision, number of iterations, operation times and extraction accuracy. In terms of the extraction accuracy, the methods made use of the evaluation methods that were widely used by line feature extraction for quantitative evaluation analysis, and compared the waterlines extracted by each algorithm and by manpower (or the actual), and then evaluated the accuracy of the extraction results from completeness (CP), accuracy (CR) and extraction quality (QL). Please refer to Literature [22] for the calculation method. Experiment 1 adopted standard edge simulation images to verify the sub-pixel extraction accuracy by the algorithm in this paper; Experiment 2 made use of QuickBird images to verify the algorithm in this paper; Experiment 3, 4, 5 and 6 made use of the panchromatic and multispectral images of Mapping Satellite to verify the algorithm in this paper, and compared and tested the waterline extraction methods proposed in [6-8].

3.1. Standard Edge Simulation Image Experiment

In order to evaluate the accuracy of the algorithm proposed by this paper simply and accurately, Experiment 1 adopted the standard edge simulation images with known extraction results for verification. Based on CCD image-forming principle, the ideal step-shaped edge[23] was formed according to the sampling theorem of square aperture, and the experiments were carried out on six standard edge images of 10°, 15°, 35°, 45°, 60° and 75°, with image size of 201×201, and the experiment results were as shown in Figure 5, and (a)-(f) were the extraction results of the above six standard image edges generated according to the method proposed in [23]by the method proposed in this paper. The extraction accuracy adopted the method proposed in [24] for quantitative calculation, which is to evaluate the extraction accuracy by average distance value of various edge points and theoretical edge line. The extraction accuracy of standard edge image at different angles by the method proposed in this paper is as shown in Table 1.

(a) Extraction of image with 10 degrees of angle (b) Extraction of image with 15 degrees of angle (c) Extraction of image with 35 degrees of angle

(d) Extraction of image with 45 degrees of angle (e) Extraction of image with 60 degrees of angle (f) Extraction of image with 75 degrees of angle

Fig.5 Accuracy Verification for Sub-pixel Extraction in Experiment 1

Table.1 Results of Different Angles Standard Image Extraction in Experiment 1

Angle of Inclination	10	15	35	45	60	75
Extraction Precision / Pixel	0.054	0.02	0.036	0.041	0.043	0.041

It can be seen from Table 1 and Figure 5 that, the extraction accuracy achieved by the method proposed in this paper can fall within 0.1pixel, indicating that the accuracy extracted by the algorithm of this paper reaches sub-pixel level. The experiments were also made for the ideal roof-style and line-type edge, which all had proved that the extraction accuracy achieved by the algorithm proposed in this paper could reach the sub-pixel level.

3.2. QuickBird Images Experiment

Experiment 2 adopted the QuickBird satellite images of Dalian region obtained in 2014 as the experimental data, with resolution of 0.61m, the size of 1173× 719 pixels, and the quad-tree segmentation results were as shown in Figure 6 below. This experiment made comparison and tested the extraction capacity of the algorithm proposed in this paper in operating efficiency, weak edges and serious concave edges. The experimental results are as shown in Figure 7 below, (a) - (c) in Figure 7 refer to the selected region of original image, the weak edge and the concave edge respectively; (d)-(f) refer to the extraction results of the original image, the weak edge and the concave edge obtained by the method proposed in [6] respectively; (g)-(i) refer to the extraction results of the original image, the weak edge and the concave edge obtained by the method proposed in [7] respectively; (j)-(l) refer to the extraction results of the original image, the weak edge and the concave edge obtained by the method proposed in [8] respectively. (m)-(o) refer to the extraction results of the original image, the weak edge and the concave edge obtained by the method proposed by this paper.

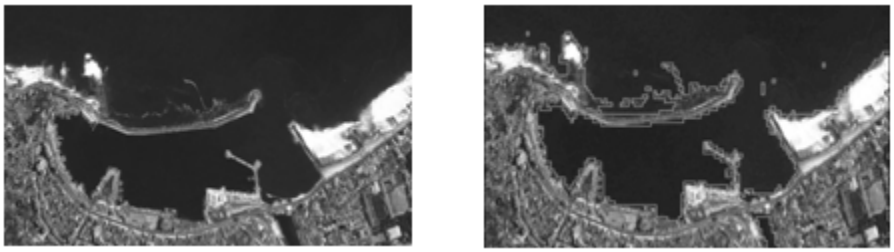

(a) Original image (b) Quad-tree segmentation results

Fig.6 Results of Quad-tree Segmentation

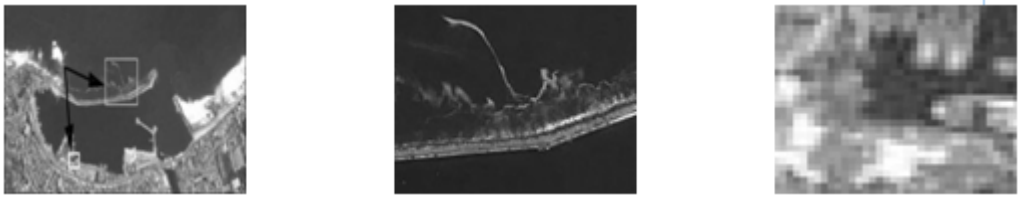

(a) Original image and selected region (b) Local selected regions (breaker interference) (c) Selected region of concave edge

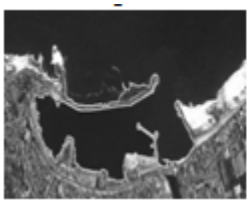

(d) Extraction by the method proposed in [6]

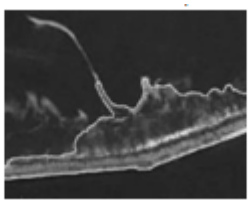

(e) Extraction of local selected region by the method proposed in [6]

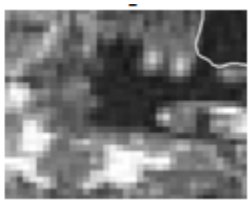

(f) Extraction of concave edge by method proposed in [6]

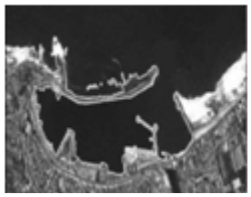

(g) Extraction by the method proposed in [7]

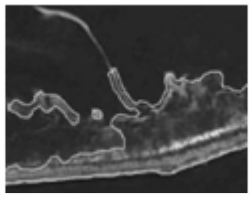

(h) Extraction of local selected region by the method proposed in [7]

(i) Extraction of concave edge by the method proposed in [7]

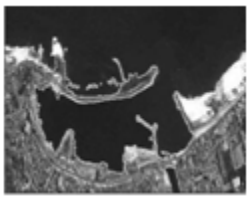

(j) Extraction by the method proposed in [8]

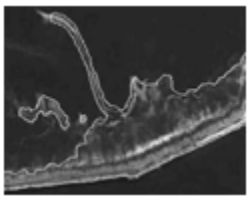

(k) Extraction of local selected region by the method proposed in [8]

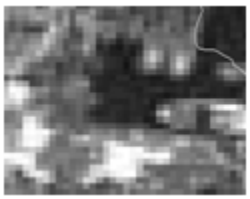

(l) Extraction of concave edge by the method proposed in [8]

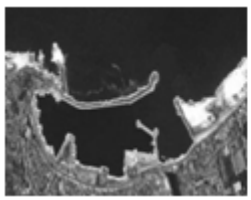

(m) Extraction by the proposed method

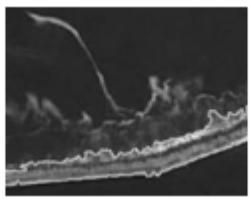

(n) Extraction of local selected region by the method

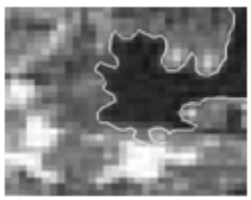

(o) Extraction of concave edge by the proposed method

Fig.7 Results of Waterline Extraction in Experiment 2

As can be seen from Figure 6, the contour obtained by quad-tree segmentation is very close to the real waterline, and provides precise initial contour for level set evolution, reduces the number of evolution and improves the efficiency of the evolution. It can be seen from the experimental results of the second column in Figure 7, the extraction edge obtained by the method specified in Literature [6-8] differed greatly from the actual edge under the interference of breaker, the extraction results were not accurate, and its capacity to extract the waterline of serious concave edges was also poor; while the method proposed by this paper has a better efficiency even under the interference of breaker, and its extraction results are closer to the actual edge, and is capable to extract the serious concave edges accurately. Meanwhile, its extraction efficiency is significantly higher than the method specified in Literature [6-8], and the statistics about the operating efficiency and extraction accuracy are as shown in Table 2.

Table.2 Operating Efficiency and Extraction Accuracy for Each Algorithm in Experiment 2

Methods	Number of Iterations/Time	Operating Time/Sec	CP/%	CR/%	QL/%
Method proposed in [6]	480	106.7	87.0	91.1	77.3
Method proposed in [7]	1940	434.5	85.0	86.3	72.3
Method proposed in [8]	430	91.5	85.0	86.3	72.3
The proposed method	140	23.4	97.4	99.4	97.0

3.3. Mapping Satellite - I Satellite Image Experiment

Experiment 3 adopted the images of Dalian region obtained by Mapping Satellite in 2014 as the experimental data, with the size of 498× 427 pixels and resolution of 2m.

This experiment made comparison and tested the extraction accuracy of the algorithm proposed in this paper in operating efficiency and general waterline. The experimental results are as shown in Figure 8 below, (a) in Figure 8 refers to the original image, (b)-(d) indicate the extraction results of the original images made according to the method specified in Literature [6-8] and in this paper respectively; (e) Enlarged image of the selected region, (f)-(h) indicate the extraction results of the selected region made according to the method specified in Literature [6-8] and in this paper respectively. The statistical results about the operating efficiency and extraction accuracy are as shown in Table 3.

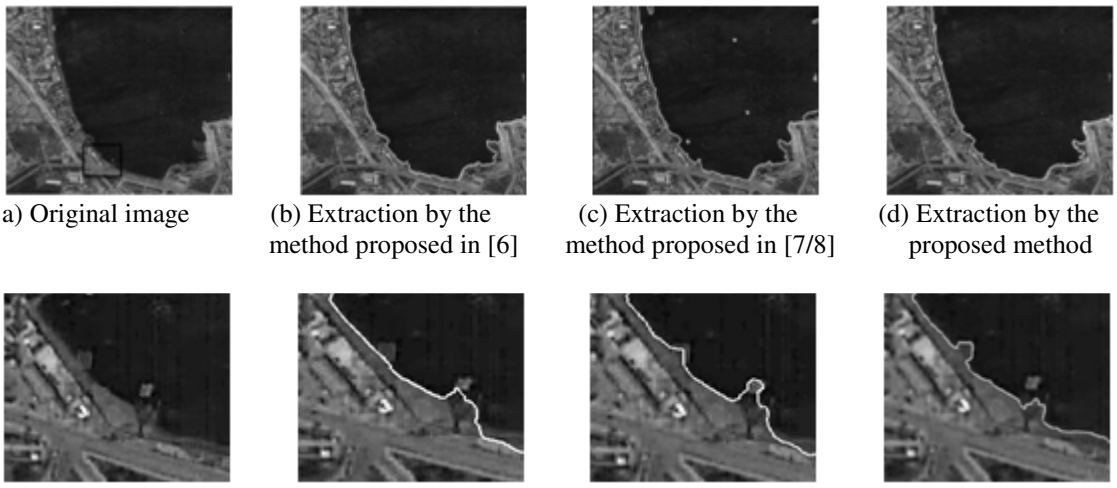

a) Original image (b) Extraction by the method proposed in [6] (c) Extraction by the method proposed in [7/8] (d) Extraction by the proposed method

e) Enlargement of the selected region (f) Extraction of selected region by the method proposed in [6] (g) Extraction of selected region by the method proposed in [7/8] (h) Extraction of selected region by the proposed method

Fig.8 Results of General Waterline Extraction in Experiment 3

Experiment 4 adopted the images of Dalian region obtained by Mapping Satellite in 2014 as the experimental data, with the size of 811×639 pixels and resolution of 2m. This experiment made comparison and tested the extraction accuracy of the algorithm proposed in this paper in operating efficiency and serious concave waterline. The experimental results are as shown in Figure 9 below, (a) in Figure 9 refers to the original image, (b)-(d) indicate the extraction results

of the original images made according to the method specified in Literature [6-8] and in this paper respectively; (e) Enlarged image of the selected region, (f)-(h) indicate the extraction results of the selected region made according to the method specified in Literature [6-8] and in this paper respectively. The statistical results about the operating efficiency and extraction accuracy are as shown in Table 4.

Table.3 Operating Efficiency and Extraction Accuracy for Each Algorithm in Experiment 3

Methods	Number of Iterations/Time	Operating Time/Sec	CP/%	CR/%	QL/%
Method proposed in [6]	200	10.6	93.0	97.0	90.0
Method proposed in [7]	680	37.4	95.8	96.2	92.1
Method proposed in [8]	140	7.3	95.8	96.2	92.1
The proposed method	60	2.5	99.7	100.0	99.7

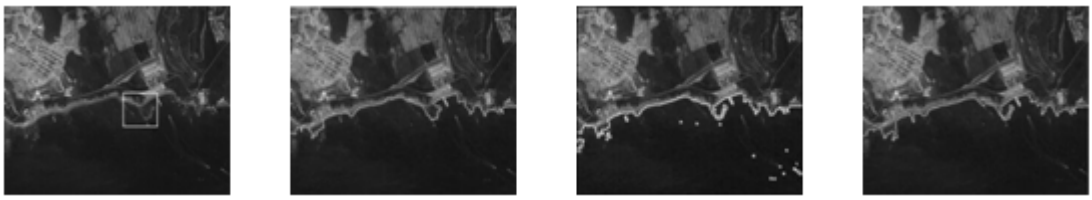

(a) Original image (b) Extraction by the method proposed in [6] (c) Extraction by the method proposed in [7/8] (d) Extraction by the proposed method

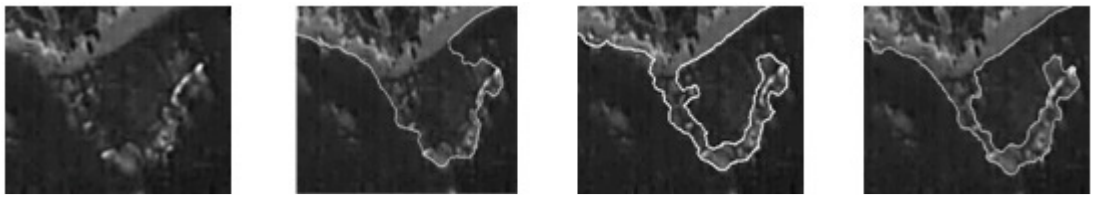

(e) Enlarged image of the selected region (f) Extraction of selected region by the method proposed in [6] (g) Extraction of selected region by the method proposed in [7/8] (h) Extraction of selected region by the proposed method

Fig.9 Experimental Results of Waterline Extraction for Concave Edges

Table.4 Operating Efficiency and Extraction Accuracy for Each Algorithm in Experiment 4

Methods	Number of Iterations/Time	Operating Time/Sec	CP/%	CR/%	QL/%
Method proposed in [6]	960	131.0	76.9	89.6	69.1
Method proposed in [7]	1020	138.6	78.7	86.6	69.3
Method proposed in [8]	900	120.6	78.7	86.6	69.3
The proposed method	220	23.2	97.4	99.0	96.2

Experiment 5 adopted the images of Dalian region obtained by Mapping Satellite in 2014 as the experimental data, with the size of 859×710 pixels and resolution of 2m. This experiment made comparison and tested the extraction accuracy of the algorithm proposed in this paper in operating efficiency and waterline of weak edges. The experimental results are as shown in Figure 10 below, (a) in Figure 10 refers to the original image, (b)-(d) indicate the extraction results of the original images made according to the method specified in Literature [6-8] and in this paper respectively; (e) Enlarged image of the selected region, (f)-(h) indicate the extraction results of the selected region made according to the method specified in Literature [6-8] and in this paper respectively. The statistical results about the operating efficiency and extraction accuracy are as shown in Table 5

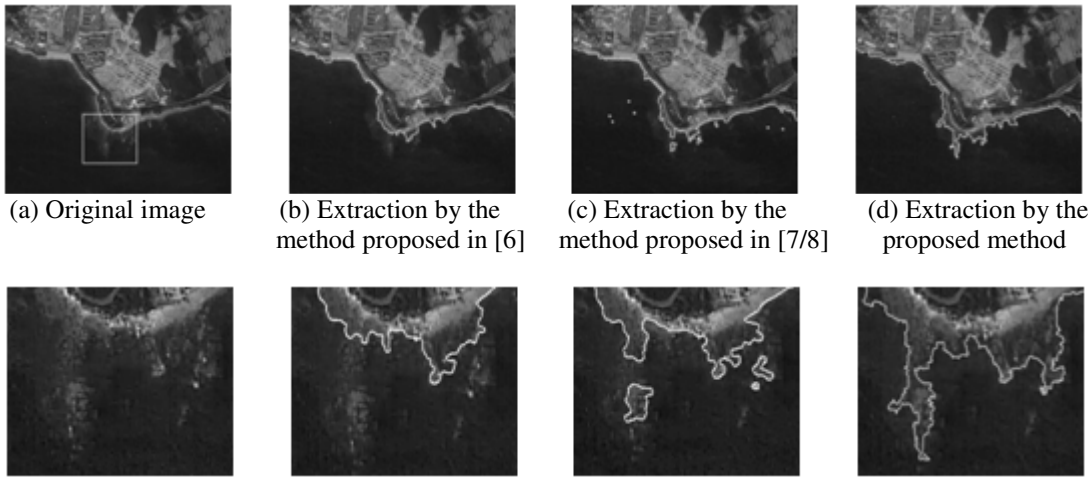

(a) Original image (b) Extraction by the method proposed in [6] (c) Extraction by the method proposed in [7/8] (d) Extraction by the proposed method

(e) Enlarged image of the selected region (f) Extraction of selected region by the method proposed in [6] (g) Extraction of selected region by the method proposed in [7/8] (h) Extraction of selected region by the proposed method

Fig.10 Experimental Results of Waterline Extraction for Weak Edges

Table.5 Operating Efficiency and Extraction Accuracy for Each Algorithm in Experiment 5

Methods	Number of Iterations/Time	Operating Time/Sec	CP/%	CR/%	QL/%
Method proposed in [6]	440	69.3	67.1	83.1	58.5
Method proposed in [7]	1740	275.8	65.8	84.5	58.9
Method proposed in [8]	420	65.2	65.8	84.5	58.9
The proposed method	100	12.2	90.8	96.1	88.2

Experiment 6 adopted the multispectral images of Mapping Satellite as the experimental data, with the size of 980×588 pixels and resolution of 10m. This experiment made comparative tests for the multispectral images. The experimental results are as shown in Figure 11 below, (a) in Figure 11 refers to the original image, (b)-(d) indicate the extraction results of the original images made according to the method specified in Literature [6-8] and in this paper respectively; (e) Enlarged image of the selected region, (f)-(h) indicate the extraction results of the selected region made according to the method specified in Literature [6-8] and in this paper respectively. The statistical results about the operating efficiency and extraction accuracy are as shown in Table 6.

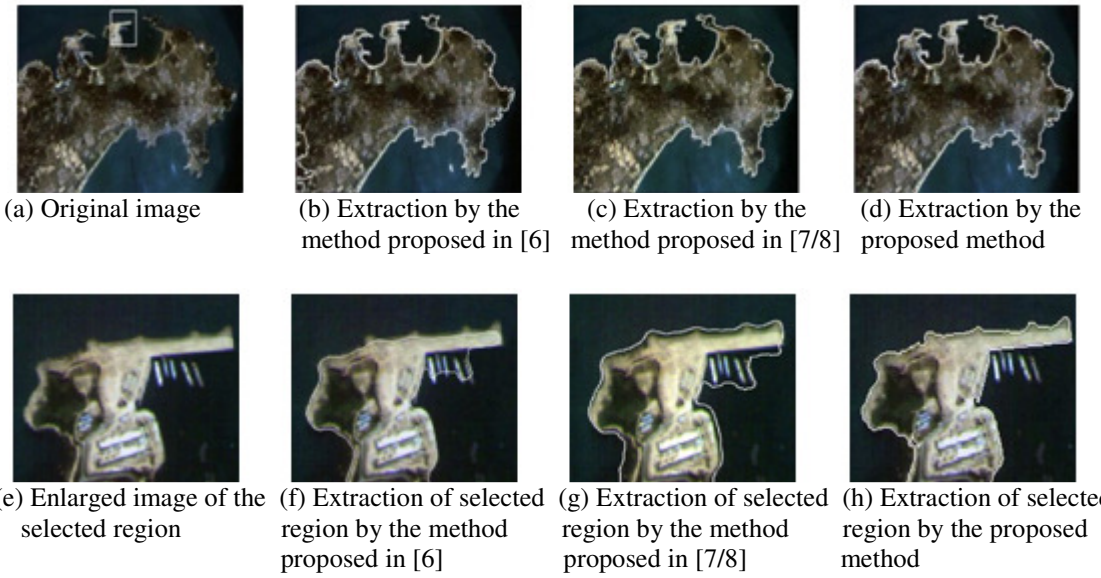

(a) Original image (b) Extraction by the method proposed in [6] (c) Extraction by the method proposed in [7/8] (d) Extraction by the proposed method

(e) Enlarged image of the selected region (f) Extraction of selected region by the method proposed in [6] (g) Extraction of selected region by the method proposed in [7/8] (h) Extraction of selected region by the proposed method

Fig.11 Experimental Results of Multispectral Image Waterline Extraction

Table.6 Operating Efficiency and Extraction Accuracy for Each Algorithm in Experiment 6

Methods	Number of Iterations/Time	Operating Time/Sec	CP/%	CR/%	QL/%
Method proposed in [6]	440	69.3	92.5	94.6	86.7
Method proposed in [7]	980	146.1	82.8	88.2	72.5
Method proposed in [8]	460	67.3	82.8	88.2	72.5
The proposed method	40	4.8	98.9	99.7	98.8

It can be seen from Figure 8, Figure 9, Figure 10 and Figure 11 that, the method proposed in this paper can extract the waterline accurately, especially the waterline of weak edges and serious concave edges, and it is featured with better stability, free from manual selection of seed points or initial boundary, with high level of automation. It can be seen from Figure 3, Figure 4, Figure 5 and Figure 6 that, the operating efficiency achieved by the method in this paper is significantly higher than that by the method specified in Literature [6-7] in terms of number of iteration and operation time, with the efficiency improved by more than 4 times; in terms of the extraction accuracy, the method proposed in this paper is higher in accuracy from 3 indicators like extraction completeness, accuracy and extraction quality.

Based on the analysis on the above 6 groups of experimental results, it can be obtained that: ①this paper utilizes the quad-tree segmentation to provide initial contour for curve evolution, realizing the automation of evolution; ②The signed pressure force function constructed in combination of the advantages of GAC, CV and LBF model has the capacity of dual-way evolution, thus improving the problem of GAC model effectively that it cannot extract the weak edges and serious concave edges at the same time, maintains the advantages of global information, avoids the minimum evolution contour locally, but also maintains the advantages of local information, so it has a better effectiveness in the segmentation of image with uneven gray scale; ③ Finally, the Selective Binary and Gaussian Filtering Level Set (SBGFRLS) method is

used to avoid reinitializing and regularization to improve the evolution efficiency; therefore, it is superior than other extraction methods in terms of efficiency and accuracy; ④The drawback lies in that the weight factor in the constructed signed pressure force function is decided by experience, which needs to be adjusted according to the details of the image and the nonuniformity of the gray scale.

4. CONCLUSIONS

In order to address the problem in waterline extraction from remote-sensing images that it is hard to extract the medium and weak edges and serious concave edges, or in long extraction time and low level of automation, this paper proposes a waterline extraction method based on quad-tree and multiple active contour models. The experimental results show that: this method can accurately extract the weak edges and serious concave edges, and owns the property of sub-pixel accuracy. Utilizes the highly efficient quad-tree segmentation method to obtain the initial contour of waterline, free from manual intervention, with high level of automation; improves the signed pressure force function and adopts Gaussian convolution and regularization level set function to avoid reinitialization, thus improving the waterline extraction efficiency significantly. As the algorithm in this paper is realized by matlab programming, the size of the image processed is limited, the larger images are considered to be divided into blocks or be processed by other methods; therefore, in-depth study will be made further in the future.

REFERENCES

[1] Lee, S.hyun. & Kim Mi Na, (2008) “This is my paper”, ABC Transactions on ECE, Vol. 10, No. 5, pp120-122.

[2] Gizem, Aksahya & Ayese, Ozcan (2009) Coomunications & Networks, Network Books, ABC Publishers.

[3] Joo-Hyung Ryu, Joong-Sun Won. Application of neural networks to waterline extraction in tidal flat from optic satellite images[C]. IEEE International Geoscience and Remote Sensing Symposium (IGARSS), 2002, 4: 2026–2028.

[4] Ping Qin. Waterline information extraction from radial sand ridge of south yellow sea[C]. The 6th International Congress on Image and Signal Processing (CISP),2013:459–463.

[5] Heng Li, Xinyu Wang. Automatic recognition of ship types from infrared images using support vector machines[C]. International Conference on Computer Science and Software Engineering, 2008, 6: 483–486.

[6] WANG Min, LUO Jiancheng, MING Dongping. Extract ship targets from high spatial resolution remote sensed imagery with shape feature [J].Information science of wuhan university ,2005,30(8):685-688.

[7] Zhen Li, Yongxue Liu, Manchun Li, etc. Automatic waterline pick-up based on improved embedded confidence[C]. The 18th International Conference on Geoinformatics,2010:1–6.

[8] ZHANG Hongwei, ZHANG Baoming, GUO Haitao. An Automatic Coastline Extraction Method Based on Active Contour Model[J]. International Conference on Geoinformatics,2013,6:111-115.

[9] SHEN Jiashuang, GUO Haitao, LI Haibin. A Water Edge Extraction Method from Images Based on Canny Operator and GAC Model[J]. Journal of Geomatics Science and Technology, 2013,30(3):264-268.

[10] GUO Haitao, SUN Lei, SHEN Jiashuang,et al. An Island and Coastal Image Segmentation Method Based on Quadtree and GAC Model [J]. Acta Geodaetica et Cartographica Sinica.2016,45(1):65-72.

[11] MinghongXie, Yafei Zhang and Kun Fu. Automatic Extraction of SAR Images Based on the Growth of Seed Points Coastline. Journal of the Graduate School of the Chinese Academy of Sciences, 2007, 24(1): 93-98.

[12] SHEN Jiashuang. Research on Technology of Equal Waterline Information Extraction and Vertical Datum Transformation in Coastal Zone [D], PLA Information Engineering University,2008.

[13] Wang X F. Level Set Method and Its Application in Image Segmentation [D]. University of Science and Technology of China, 2009 .().

[14] Chan T F, Vase L A. Active contours without edges [J]. IEEE Transactions on Images Precessing.2001,10（2）：266-277.

[15] Li C, Kao C Y, Gore J C, et al. Implicit active contours driven by local binary fitting energy[C]//Computer Vision and Pattern Recognition, 2007. CVPR'07. IEEE Conference on. IEEE, 2007: 1-7.

[16] Li C, Kao C, Gore J C, et al. Minimization of region-scalable fitting energy for image segmentation. IEEE Transactions on Image Processing.2008,17(10):1940-1949.

[17] Yun T, Mingquan Z, Fuqing D, et al. Efficient active contour model driven by statistical and gradient information[J]. Journal of Image and Graphics, 2011,16(8): 1489-1496.

[18] Zhang K, Zhang L,Song H, et al. Active contours with selective local or global segmentation: a new formulation and level set method[J]. Image and Vision computing, 2010, 28(4): 668-676.

[19] Wang X F, Min H. A level set based segmentation method for images with intensity inhomogeneity[M]//Emerging Intelligent Computing Technology and Applications. With Aspects of Artificial Intelligence. Springer Berlin Heidelberg, 2009: 670-679.

[20] Su Rina, Wu Jitao. Refion-based Active Contour Model Improving The Signed Pressure Force Function[J].Journal of Image and Graphics ,2011,16（12）：2169-2174.

[21] Fedkiw R, Osher S. Level set methods and dynamic implicit surfaces[J].Springer-Verlag, NewYork, 2002, 44: 77.

[22] Y.Shi,W.C.Karl, Real-time tracking using level sets, IEEE Conference on Computer Vision and Pattern Recognition.(2005)34–41.

[23] Zhang K, Song H, Zhang L. Active contours driven by local image fitting energy[J]. Pattern Recognition,2010,43 (4):1199- 1206.

[24] DING Lei, YAO Hong,GUO Haitao, ,et al. Using Neighborhood Centroid Voting to Extract Road Centerline from High Resolution Image[J]. Journal of Image and Graphics,2015,20(11):1526-1534.

[25] HE Zhonghai, WANG Baoguang, LIAO Yibai. Study of Method for Generating Ideal Edges[J].Optics and Precision Engineering,2002,10(1):89-93.

[26] CHEN Xiaowei, XU Zhaohui, GUO Haitao,et al. Universal Sub-pixel Edge Detection Algorithm Based on Extremal Gradient[J]. Acta Geodaetica et Cartographica Sinica,2014,43(5):500-507.

AUTHORS

Zhang Baoming (1961-). He is currently a full professor at Department of Photogrammetry and Remote Sensing, Zhengzhou Institute of Surveying and Mapping. His research interests are in the areas of digital photogrammetry, remote sensing, image processing, and pattern recognition.
Email: zbm1960@163.com

Guo Haitao (1976-), Ph.D. He is currently an associate professor at Department of Photogrammetry and Remote Sensing, Zhengzhou Institute of Surveying and Mapping. His main research interests include multi-temporal image processing and machine learning with applications to remote sensing image analysis.
Email: 15515768676@163.com

Lujun (1981-), Ph.D. He is currently a Lecturer at Department of Photogrammetry and Remote Sensing, Zhengzhou Institute of Surveying and Mapping. His research interests are related to digital photogrammetry and computer vision.
Email: ljhb45@126.com

Yu Jintao (1992-). He is currently a Master Degree Candidate at Department of Photogrammetry and Remote Sensing, Zhengzhou Institute of Surveying and Mapping. His research interests are related to object recognition from remote sensing images.
Email: 289386886@qq.com

PARTIAL HARQ RETRANSMISSION FOR BROADCAST IN FADING CHANNELS

Belkacem Mouhouche, Louis Christodoulou, Manuel Fuentes

Samsung Research & Development UK,
Staines-Upon-Thames, TW18 4QE, UK

ABSTRACT

In this paper, we study the feasibility of a hybrid scheduling approach for broadcast systems in frequency selective fading channels. The hybrid scheduling approach consists of two components: a first broadcast component and a second unicast component. The unicast component is activated if the mobile fails to correctly decode the packet and thus sends back a negative acknowledge to the base station. In this paper, we show that there is an optimal modulation and coding schemeto be used for each one of the components presented. The broadcast optimal modulation and coding scheme depends on the best alignment in fading between different receivers. On the other hand, the unicast optimal modulation and coding scheme depends on the particular fading profile of each mobile separately.

KEYWORDS

Point-to-multipoint, broadcast, incremental redundancy, ACK/NACK, HARQ process

1. INTRODUCTION

Broadcast systems are used as an efficient way to deliver data to users interested in the same content within a geographical location with a very low marginal cost per user. Digital television systems such as Digital Video Broadcasting–2ndGeneration Terrestrial (DVB-T2) [1] or Advanced Television System Committee – 3rd Generation (ATSC 3.0) [2] only support downlink transmissions. For instance, in DVB-T2 the receiver uses synchronization signal to detect the presence ofDVB signals. Layer 1 Signaling is then used to detect the different programs within the OFDM signal (called Physical Layer Pipes, PLPs). The transmitter on the other side is not even aware of the presence of the receiver. There is no uplink system that allows the use of any positive/negative acknowledgement of reception. The system is designed from the beginning to be able to reach users on the cell edge. This kind of system suffers from a "race to the bottom" effect because the scheduler needs to select a Modulation and Coding Scheme (MODCOD), or equivalently a data transmission rate that is decodable by all users. Thus, the lowest data rate is applied to all users; even those that have good channel conditions and are able to support a higher data rate.

Broadband cellular systems, such as 3G and 4G, are designed to deliver high data rates to users in a unicast mode. These systems also have native support for broadcast components such as Multimedia Broadcast Multicast System (MBMS) [3] and enhanced Multimedia Broadcast Multicast System (eMBMS) [4]. Unlike DVB, 3G and 4G systems have the possibility to transmit to a subgroup of users in the same cell using multicast. In this case, the base station is aware of the presence of receivers, but no uplink transmission is used to report positive and negative acknowledgements. The transmitter once again builds on the weakest receiver in the multicast

Natarajan Meghanathan et al. (Eds) : CSITA, DMAP, ISPR, NMCO - 2017
pp. 35– 44, 2017. © CS & IT-CSCP 2017 DOI : 10.5121/csit.2017.71404

group since the MODCODmust be low to ensure the correct reception of all the packets by all receivers.

Since more and more TV terminals are equipped with a broadband connection, a novel Redundancy on Demand (RoD) technique was proposed recently in order to improve the reception of terrestrial broadcast signals with the help of additional redundancy data [5]. Depending on the terminal position and quality of reception, a parallel redundancy transmission on the broadband connection can help to increase reception quality and network coverage.

2. BROADCAST/UNICAST REPARTITION

In case of 5G, the terminals receiving a broadcast/multicast transmission also have broadband (one to one) connections with the base station. A possible improvement would be to consider an uplink transmission of negative acknowledgements incase the receiver does not correctly decode the packet. This can be done by adding a Hybrid Automatic Repeat Request (HARQ) process, in which the first transmission is not in a point-to-point mode but in a broadcast mode. Once this broadcast detection fails,a negative acknowledge (NACK) is transmitted and the HARQ process takes over the retransmission and decoding of this packet by using, for instance, incremental redundancy. The advantage of this type of schemes is that the base station does not need to build on the weakest receiver in the multicast group. It may be more advantageous to use a higher modulation and coding scheme, even if some of the transmissions need to be repeated for only few users.

The scheduler selects one transmission rate to satisfy the maximum number of users. However, users near the cell edge experience bad channel quality due to power attenuation. In this case, the scheduler can choose between two extreme cases: either to use a data rate that fits the good channel quality cluster or to use a low data rate that can be decoded by all users, including the ones at the cell edge. The former case excludes users at the cell edge; the latter case is inefficient because a low data rate is imposed on all users. The goal of this paper is to find the best compromise to maximize the delivery time.

The total time needed to deliver a correct packet to all users is given by a sum of the time needed for the broadcast phase and the time needed for the unicast (retransmission) phase. The retransmission time depends on the number of frequency resources allocated to the HARQ process. For simplicity, it is assumed that the same number of resources is allocated to both the broadcast and the HARQ components.

In an ideal scenario, where all users have the same channel quality, the base station can choose a retransmission rate that guarantees reception for all users. As the supported data rates across users may vary, it is difficult for the base station to find a rate that fits all users, unless it selects the lowest rate that all users can decode. However, this penalizes users with good channel conditions and increases the total delivery time. In this paper, we present an optimization algorithm that selects the best data rate based on the channel qualities of the users. We also present simulation results that show the gain in delivery time that can be obtained by using an HARQ component.

3. SYSTEM MODEL

In this manuscript, a single cell scenario using multicarrier transmissionswith Orthogonal Frequency-Division Multiplexing (OFDM) is considered. It is assumed that mobile receivers are located randomly within the cell. Receivers suffer both from slow fading due to attenuation and shadowing as well as fast fading. Receivers close to the base station will have a better signal-to-

noise ratio (SNR) than users on the cell edge. We assume that the base station has knowledge of all user channels for each subcarrier, for example via Channel Quality Indicators (CQI).

A mixed broadcast/multicast protocol divided into two steps is considered, as shown inFig. 1. In a first broadcast step, the base station transmits a packet to all users using the same carrier (group of adjacent subcarriers) frequency. Some users will be able to decode the packet and transmit a positive acknowledgement (ACK), whereas some other users will not be able to decode the packet and shall transmita NACK. In a second step, the base station addresses the users that transmitted a negative acknowledge using unicast. Each user can be addressed with a suitable (robust) MODCOD that will enable it to decode the packet after one retransmission.

It is also necessary to consider the problem of optimizing the frequency time resources used for a complete transmission of one packet to all users. In such case, at each time, one frequency resource (subcarrier) is used. Hence, this amounts to optimizing the total time to deliver a correct packet to all users. The total time is given by Eq. (1).

$$T_{\text{total}} = T_{\text{bc}} + T_{\text{uc}} \tag{1}$$

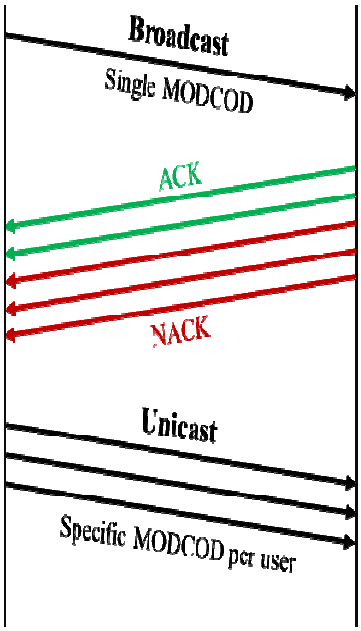

Fig. 1. Mixed broadcast/multicast protocol with retransmissions.

The system selects a single MODCOD for the broadcast phase, corresponding to a rate R_{bc}. For example, if a 16QAM modulation (4 bits per symbol) is used with coding rate 10/15, the rate is calculated as$R_{\text{bc}} = 4 \cdot \frac{10}{15} = 2.66$ bps. In the second phase, following reception of one or more NACKs, the system selects a unique and specific MODCOD for each user that failed to decode the broadcast packet, thus proceeding to retransmit the packet in a unicast manner. The MODCOD selected for user *i* results in rate R_i. For each user *i*, the retransmission does not occur all the time but rather only a fraction BER(*i*), where BER is the bit error rate. For example, if the BER of a given user is 0.1 then retransmission occurs only 10% of the time. Thus the total unicast time is given by Eq. (2), and the total time to deliver 1 bit is given by Eq. (3).

$$\sum_{i=1}^{N_{\text{users}}} \text{BER}(i) \cdot \frac{1}{R_i} \tag{2}$$

$$T_{\text{total}} = \frac{1}{R_{\text{bc}}} + \sum_{i=1}^{N_{\text{users}}} \text{BER}(i) \cdot \frac{1}{R_i} \tag{3}$$

4. PHYSICAL LAYER MODEL

The latest PHY layer specification of ATSC 3.0 [2] is used in order to calculate the BER of the initial transmission and subsequent retransmissions. The main part of the ATSC 3.0 PHY layer is the Bit Interleaved Coded Modulation (BICM) chain consisting of a Forward Error Correcting (FEC) code, a bit interleaver and a constellation mapper [6, 7]. The FEC adopted in ATSC3.0 is a Low-Density Parity Check (LDPC) code with two possible block code lengths: short code 16200 and long code 64800 [2]. In this paper, we only consider the long code case. The constellation mapper uses the Non-Uniform Constellationsproposed in [7], whichare optimized for a particular code rate. Bit interleavers are also optimized to achieve a very good spectral efficiency. In ATSC 3.0, coding rates from 2/15 to 13/15 with step 1/15 are used. Constellation orders to use are: QPSK, 16QAM, 64QAM, 256QAM, 1KQAM and 4KQAM. As an example,Fig. 2 shows the waterfall SNR performance vs. BER for a 16QAM and coding rates ranging from 5/15 to 13/15, for AWGN channel.

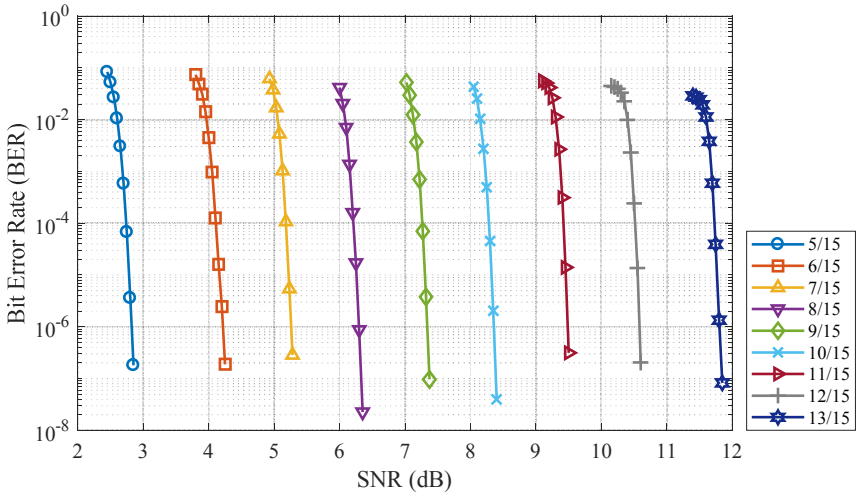

Fig. 2. SNR vs. BER of ATSC3.0, for modulation size 16QAM and AWGN channel model.

From Fig. 2, it is possible to affirm that both spectral efficiency and SNR performancedepend on the selected MODCOD. The spectral efficiency of the system ranges from 0.266 bps/Hz for QPSK with coding rate 2/15 to 10.4bps/Hz for 4KQAM with coding rate 13/15. This range is shown in Fig. 3.

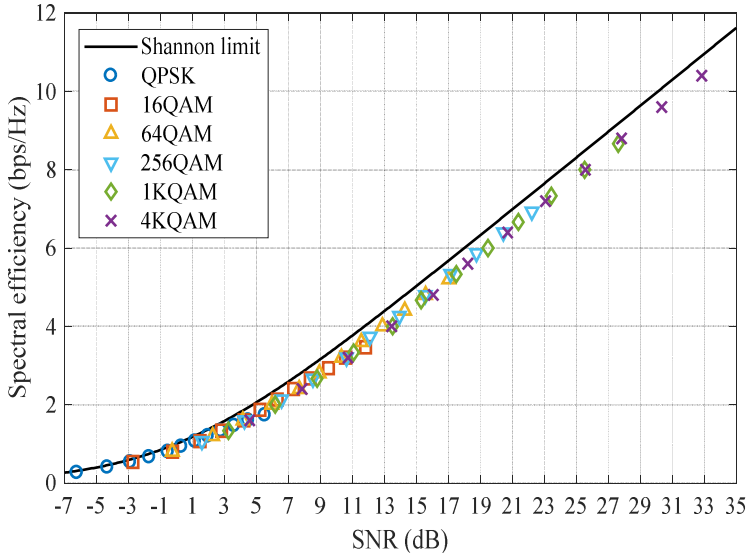

Fig. 3. Spectral efficiency vs. SNR of ATSC3.0 chain, for AWGN channel model.

The horizontal axis represents the SNR needed to achieve a particular efficiency. This corresponds to the waterfall (BER<10^{-6}) of the corresponding MODCOD. For example, it takes around 33dB of SNR to use the MODCOD 4K with code rate 13/15.

The scheduler selects a given MODCOD for the first transmission (broadcast phase) and then a possibly different MODCOD for each user requiring a retransmission. A high MODCOD selected at the first phase allows the broadcast transmission time to be minimized. However, the higher the MODCOD, the larger the number of users transmitting NACK signals. As a result, this will increase the number of users that require a retransmission in the unicast phase. It will also increase the BER of each user. Thus a selection of a higher MODCOD for the broadcast phase will reduce the first term of Eq. (3),$\frac{1}{R_{\mathrm{bc}}}$, and increase the second term $\sum_{i=1}^{N_{\mathrm{users}}} \mathrm{BER}(i) \cdot \frac{1}{R_i}$, both in the number of users inside the sum and the BER that multiplies each user time. The optimization is focused on finding the best compromise between the first and the second term. Note that the second unicast phase is used in the time calculation but it is entirely dependent on the broadcast MODCOD.

5. FREQUENCY-SELECTIVE CHANNELS

In the case of frequency selective channels, the scheduler responsible for implementing the mixed broadcast/unicast protocol has two different tasks. The first task is to select the carriers to be used for each step; and the second task is to select the MODCOD for each step. In order to select the best set of carriers, the scheduler needs to select the best carriers across all users. This is achieved by avoiding deep fades across any of the users, since it will limit the MODCOD used.

Fig. 4 shows an example of 3 users experiencing different fading at a given time instant. The selection of any of the particular carriers (A, B, C) will lead to a very bad choice of modulation and coding scheme. The best choice is to select the carrier that allows the use of the highest possible MODCOD, in order to minimize the transmission time of the broadcast component, as shown in Fig. 4 (D). This is achieved by taking theminimum SNR across users for each carrier, then locating the maximum of these SNRs. This “max-min” approach for carrier selection will be used for the first transmission. If the fading for user i at subcarrier c is defined asSNR(i,c), then the best subcarrier to be used for the broadcast case is given by Eq. (4).

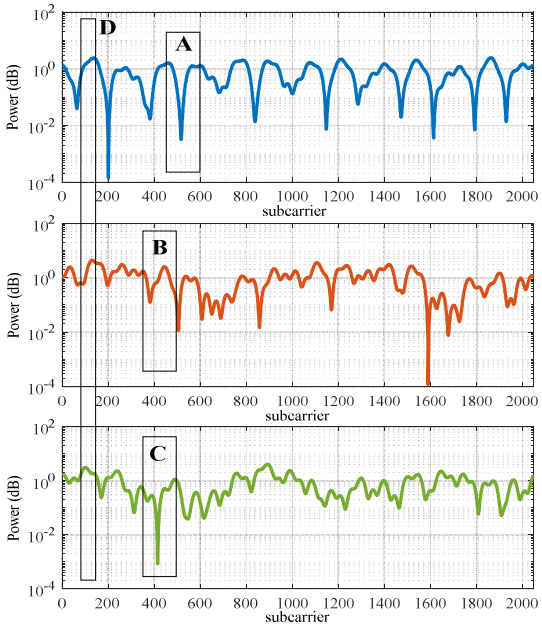

Fig. 4. Frequency selective channels of 3 users and best carrier for broadcast.

$$\text{best} = \max_{subcarrier\ c} \left(\min_{user\ i} \text{SNR}(i, c) \right) \tag{4}$$

Depending on the expected average throughput of the broadcast content the scheduler can user more than one carrier to deliver the content. The max-min equation can then be used in the same way but across adjacent carriers.

6. SIMULATION RESULTS

In order to analyze the total time needed for the content delivery using the two step protocol, we consider a single cell system where users are randomly located inside the cell. The fading suffered by each user is composed of two components: a slow fading component related to the attenuation (path-loss and shadowing) due to the mobile location and shadowing and a fast fading component, due to the multipath selective channel experienced by each mobile. The slow fading parameters are given in Table 1. A 'pedestrian B' channel is used for the fast fading component, with a delay profile as defined in Table 2.

Table 1. Slow fading parameters used in the simulations.

Parameter	**Value**
Number of subcarriers	2048
Path-loss propagation model	Macro cell: urban Area [9]
Shadowing standard deviation	8
eNB Power	1 Watt
Cell Radius	1000m
MinimumUE distance from eNB	50m
Subcarrier spacing	15KHz
Thermal Noise	-173 dBm

Table 2. 'Pedestrian B' channel.

Relative Delay (ns)	0	200	800	1200	2300	3700
Power (dB)	0	-0.9	-4.9	-8.0	-7.8	-23.9

The objective is to assess the total time needed for the delivery of 1 bit/Hz and study the best MODCOD scheme to be utilized during the broadcast step. Furthermore, we aim to find the best compromise allowing us to minimize the overall transmission time (the sum of the broadcast and unicast times). From Fig. 3, it is possible to affirm that spectral efficiencies of some MODCODs are overlapping. The study can be further simplified by considering only coding rates 6/15, 7/15, 8/15, 9/15, 10/15, 11/15, 12/15, 13/15 for modulation sizes 16QAM, 64QAM, 256QAM, 1KQAM and 4KQAM. For the low modulation (QPSK) we also consider low code rates including 2/15, 3/15, 4/15 and 5/15, since these codes are the only ones that give a very low spectral efficiency. The study covers 52 MODCODs ranging from QPSK2/15 to 4KQAM13/15.

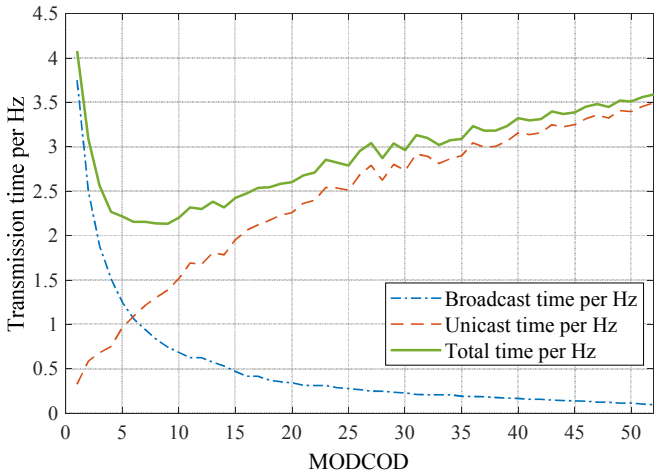

Fig. 5. Time per Hz to deliver 1 bit to all users in a cell with 15 users.

We start by considering a cell with 15 users suffering fading as explained above. The broadcast time, the unicast time and the total time are depicted in Fig. 5. The total time is composed of two components: the broadcast and unicast time, which decreases and increases with the MODCOD respectively. The broadcast time decreases because the data rate increases with the MODCOD, and thus the time needed to transmit a certain amount of information decreases. On the other hand, as the MODCOD (of the broadcast phase) increases, the unicast step sees time increase. This is due to the fact that more and more users are requesting NACKs and thus the total time taken to service these increases. The interesting conclusion resides in the total minimum time. From the figure, it is observed that the MODCOD 9, i.e. QPSK 10/15, guarantees the minimum transmission time. For the unicast phase, the scheduler selects the best available carrier and uses the best MODCOD that guarantees an error free transmission (BER curve waterfall below the carrier SNR).

This study can be extended by evaluating the best MODCOD and the percentage of NACK transmitting users in order to draw conclusions on which strategy to use depending on the cell load. The results are given in Fig. 6.

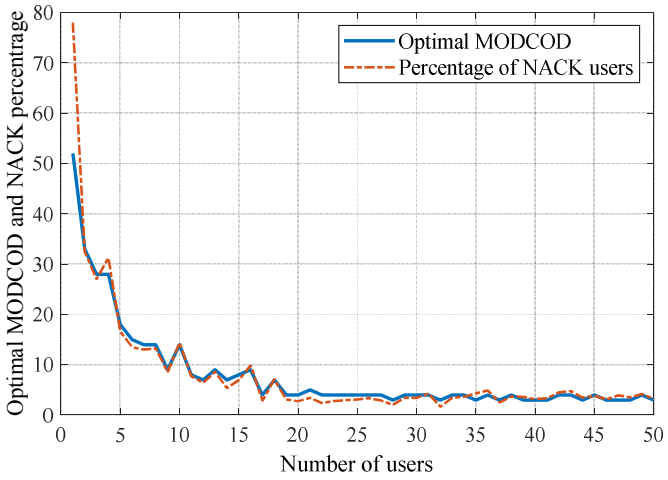

Fig. 6. Optimal MODCOD scheme and percentage of NACK users.

The optimal MODCOD decreases as the number of users increases. This is due to the necessity to use a more conservative approach when covering a highernumber of users. The same thing is observed from the NACK percentage (the number of users that require retransmissions) that decreases with the MODCOD. For lower number of users, a more aggressive approach is more optimal as it delivers the broadcast message in a very short time using a high MODCOD. Users that do not receive the message will be addressed by unicast. The percentage of users is high, but since the total number of users in the cell is low, the number of users to be addressed by unicast also remains low. This guarantees that the total sum of broadcast and unicast subsequently remains low.

7. CONCLUSIONS

In this paper, we propose a new hybrid approach for content delivery in frequency selective fading channels. The proposed method is based on two components: broadcast and unicast (HARQ retransmission) components. The broadcast component is used to deliver the content to the users in a first phase, whereas the HARQ component is used to retransmit the same packet to users that did not receive it during the broadcast phase. The advantage of this approach is that it frees up the scheduler from trying to select a uniquetransmission data rate for all users with some users having bad channel qualities. We show that usinga conservative approach that serves all the users in oncetransmission is not optimal. In order to reduce the total transmission time, there is an optimalMODCOD for both stages. For cells with moderate numbers of users the optimal MODCOD is in the mid-range representing the best balance between the two stages. For cells with a high number of users a conservative approach consisting in the choice of a low MODCOD is preferable, in order to reduce the number of users that will require retransmissions.

ACKNOWLEDGEMENTS

This work was supported in part by the European Commission under the 5GPPPproject 5G-Xcast (H2020-ICT-2016-2 call, grant number 761498). The viewsexpressed in this contribution are those of the authors and do not necessarily represent the project.

REFERENCES

[1] Digital Video Broadcasting (DVB); frame structure, channel coding and modulation for a second generation digital terrestrial television broadcasting system (DVB-T2) ETSI EN 302 755, V1.1.1, 2008.

[2] L. Fay, L. Michael, D. Gomez-Barquero, N. Ammar, and W. Caldwell, "An overview of the ATSC 3.0 physical layer specification," IEEE Transactions on Broadcasting, vol. 62, no. 1, Mar. 2016.

[3] V. Vartiainen and J. Kurjenniemi, "Point-to-multipoint multimedia broadcast multicast service (MBMS) performance over HSDPA," in Personal, Indoor and Mo bile Radio Communications, 2007. PIMRC 2007. IEEE 18th International Symposium on, Sept 2007, pp. 1–5.

[4] D. Lecompte and F. Gabin, "Evolved multimedia broadcast/multicast services (eMBMS) in LTE-advanced: overview and rel-11 enhancements," IEEE Communication Magazine, vol. 50, no. 11, pp. 68-74, November 2012.

[5] J. Qi, J. Zoellner, J. Robert, L. Stadelmeier, and N. Loghin, "Redundancy on demand – extending the coverage area of terrestrial broadcast via broadband networks," IEEE Transactions on Broadcasting, vol. 61, no. 3, pp. 337–345, Sept. 2015.

[6] A. Martinez, A. Fabregas and G. Caire, "Bit-interleaved coded modulation," Found. Trends Comm. Inf. Theory, vol. 5, no. 1-2, pp. 1–144, 2008.

[7] L. Michael and D. Gomez-Barquero, "Bit-Interleaved Coded Modulation (BICM) for ATSC3.0", IEEE Transactions on Broadcasting, Vol: 99, January 2016.

[8] B. Mouhouche, D. Ansorregui, A. Mourad "Higher Order Non Uniform Constellations for Broadcasting UHDTV", IEEE Wireless Communications and Networking Conference (WCNC) 2014.

[9] 3GPP TR 36.942, "Radio Frequency (RF) system scenarios," Release 11, Sept. 2012.

AUTHORS

Belkacem Mouhouche received his Ph.D. degree in Signal Processing from EcoleNationaleSuperieure des Telecoms (Telecom Paristech) in France in 2005. During his Ph.D. he worked on 3GPP third generation systems (UMTS), he later worked as a 3GPP standard Engineer following the development of HSDPA and LTE systems. He was also involved in FP7 European Project End to End Efficiency (E3) where he worked on cognitive radio in heterogeneous systems. Before joining Samsung he worked in major telecommunication companies like Sierra Wireless, Freescale Semiconductor, NEC and Alcatel Lucent. His research interest are in the area of advanced techniques for the physical layer of future communication systems including MIMO, beamforming and coding applied to broadcast and broadband systems like the LTE-A and DVB, ATSC3.0. Recently, He was heavily involved in the development of the latest broadcast terrestrial standard ATSC3.0 and lead the broadcast activity within the 5G-PPP project Fantastic-5G. Recently, he was appointed as innovation and dissemination manager of the 5G-PPP project 5G-Xcast focused on new point to multipoint techniques for 5G networks.

Louis Christodoulou received his Ph.D. degree in electronic engineering from the University of Surrey, U.K., in 2016, focussing on the development of a hybrid unicast broadcast enhanced multimedia delivery framework over LTE. His current research interests include multipoint transmission techniques and with experience working in the television broadcast industry; future multimedia content delivery, mobile broadcast, and radio resource management. He is currently a 5G Research Engineer with Samsung Electronics Research and Development Institute, U.K. contributing to

the Horizon 2020 5GPPP European Projects such Fantastic-5G focused on 5G PHY solutions and 5G-Xcast focused on point to multipoint solutions for 5G.

Manuel Fuentes received his M.Sc. degree in telecommunication engineering and a second M.Sc. degree in communication technologies, systems and networks from the Universitat Politecnica de Valencia, Spain, in 2012 and 2013, respectively. He also obtained the Ph.D. degree in telecommunication engineering in 2017. From 2012 to 2017, he was working at the Institute of Telecommunications and Multimedia Applications (iTEAM). He also has been a guest researcher at the Vienna University of Technology, Austria, in 2016. He participated in several R&D projects where his research interests were focused on interference mitigation and network planning activities between digital broadcasting and 4G technologies. He also has contributed actively to the ATSC 3.0 standardization process. In 2017, Dr. Fuentes joined the Samsung Electronics R&D UK team as a 5G research engineer to participate in the 5P-PPP phase-2 project 5G-Xcast, for the efficient delivery of broadcasting in 5G New Radio. His main research interests include physical layer procedures, innovative techniques in bit-interleaved coding and modulation, and multi-antenna communications

ASTRONOMICAL OBJECTS DETECTION IN CELESTIAL BODIES USING COMPUTER VISION ALGORITHM

Md. Haidar Sharif[1] and Sahin Uyaver[2]

[1]International Balkan University, Republic of Macedonia
[2]Turkish-German University, Turkey

ABSTRACT

Computer vision, astronomy, and astrophysics function quite productively together to the point where they are completely logical for each other. Out of computer vision algorithms the progress of astronomy and astrophysics would have slowed down to reasonably a deadlock. The new researches and calculations can lead to more information as well as higher quality of data. Consequently, an organized view on planetary surfaces can change all in the long run. A new discovery would be a puzzling complexity or a possible branching of paths, yet the quest to know more about the celestial bodies by dint of computer vision algorithms will continue. The detection of astronomical objects in celestial bodies is a challenging task. This paper presents an implementation of how to detect astronomical objects in celestial bodies using computer vision algorithm with satisfactory performance. It also puts forward some observations linked among computer vision, astronomy, and astrophysics.

KEYWORDS

Algorithm, Astrophysics, Astronomy, Computer Vision, Crater, Detection

1. INTRODUCTION

The detection of astronomical objects in celestial bodies using the techniques of computer vision is not new. Many researches, related to astronomy and astrophysics focused around computer vision, have been performed [1-7]. Takahashi et al. [1] mainly focused on spectro-polarimetry of reflected light from exoplanets which was anticipated to be a powerful method for analyzing atmospheric composition and atmospheric structure. Their concept is one of the more fascinating aspects of using computer vision algorithms for defining features of an exoplanet to analyze of its atmosphere. After establishing analytically derived error formulas the outcome is the estimation for a number of planets, where detection of water vapor is possible. This leads to the resulting calculations of a relatively high number of searches for planets that are possibilities. Explicitly, the characterization of planetary atmospheres using spectro-polarimetry is genuinely possible with an ELT (Extremely Large Telescope) and a direct observing spectro-polarimeter. A healthy amount of an important discovery on survivability of exoplanets came from the TRAPPIST-1 system which made it possible to characterize potentially habitable planets orbiting a nearby ultra-cool dwarf star. Bourrier et al. [2] described the method of performing a four-orbit reconnaissance with the space telescope imaging spectrograph located on the Hubble space telescope which in turn allows the study of the stellar emission at Lyman-α. The Lyman-α line is a spectral line of one-electron ions in the Lyman series which is emitted when the electron

Natarajan Meghanathan et al. (Eds) : CSITA, DMAP, ISPR, NMCO - 2017
pp. 45– 52, 2017. © CS & IT-CSCP 2017 DOI : 10.5121/csit.2017.71405

declines from the principal quantum number being two orbital to the principal quantum number being one orbital. However, their study assesses the presence of hydrogen exospheres around the two inner planets and it determines their ultraviolet irradiation. The lack of proper database management in the gathering of astronomical data as the images and other aspects of databases in astronomy can be large and inefficient. But Erkeling et al. [3] suggested and resolved on the issue at hand. The work of Romano et al. [4] is among the interesting aspects of computer vision in astronomy, as it focused on stellar information which in turn can affect every other astronomical object. They introduced an application of support vector machines (SVMs) that can identify potential supernovae using photometric and geometric features computed from astronomical imagery. Nagel et al. [5] and Upadhyay et al. [6] focused strictly on analysis of surfaces. Nagel et al. [5] discussed general aspect that can be applied to astronomical imagery. Upadhyay et al. [6] used established algorithms and applied them to the surface of the moon to detect craters. To create an encompassing aspect, Nakajima et al. [7] tied to do the spectro-polarimetric characterization of exoplanetary atmospheres. They introduced a method of molecular line spectroscopy of M dwarfs. Carbon and oxygen abundances are derived, respectively, from CO and H_2O lines in the K band which is then applied to Gliese 229A, the primary star of the brown dwarf companion, and Gliese 229B. All of the aforementioned works have separate algorithms which lead to a specific result using astronomical data of more than one simple nature. The goal is to ideally incorporate these parts as a solution to exoplanetary research in general. This incorporation would mean that further work would use a limited amount of data to characterize an astronomical object. For example, an exoplanet using aspects like spectro-polarimetry and spectroscopy, while objectively it could analyze the surface [8] of the object if the data were more meticulous. There are many algorithms which would be implemented as part of the resulting entity.

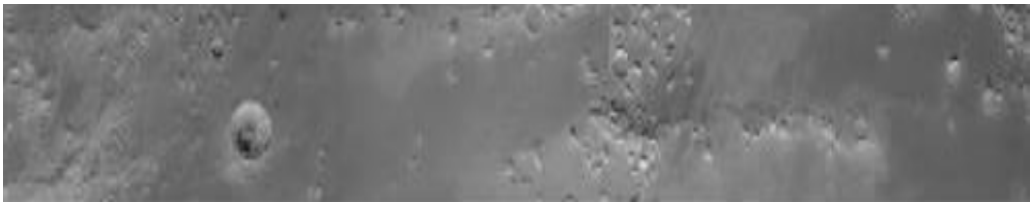

Figure 1. How to detect the number of craters from this sample image of the planet of Mars?

Crater is one of the key astronomical objects in celestial bodies. Crater detection is one of the key interests of many computer vision researchers [9-11]. Craters provide key information on planet formation. Statistical information of the size and number of craters help in determining the geological age of a planetary surface. Detection of craters is challenging because they come in all shapes and sizes. Size is one of main problems, as some craters could be a few pixels wide while others could be hundreds of pixels wide. Craters can be inside of other craters. Color of the craters can play a dramatic role. Different celestial bodies usually have different surface colors. For instance, the Mars is more orange and red in color while its moon the Phobos is greyer in color. Shades of craters play an important role, i.e., craters can contain shades due to neighboring hills or mountains. Such craters have been proven to be the hardest to detect. Various methods for detecting craters autonomously using computer vision have been applied but the methods have a high error percentage and the images from various satellites differ a lot from one another along with their thresholding conditions. For instances, Honda et al. [9] added a variant of the genetic algorithm to form a candidate of craters before using a self-organizing mapping to categorize the craters from non-craters. Meng et al. [10] constructed candidate areas that might contain craters. Their method represented a boost in performance. However, Hough transforms are essential in the algorithm used for this variant of autonomous crater detection. Viability becomes a problem when the craters do not contain a clear edge, resulting in false positives. Mu et al. [11] used ideas from biology to detect craters on celestial bodies. Craters do have some features like cells and they

attempted to try cell algorithms on crater detection. The cells, on which the algorithm was applied prior, were complex cells of the human cortex. As with cells, the craters were subjected to a variant of an approach that strives to improve the Haar like features, which contain gradient texture information. Hence it is making easier to detect them in the long run.

In this paper, we are more interested to focus on crater detection in celestial bodies. Figure 1 demonstrates a sample image of the planet of Mars. We wish to detect the number of craters exist on this image. How can we detect the existing creators in this image? We have implemented an algorithm based on circular Hough transformation to detect craters. The algorithm constructs candidate objects that resemble the looked-for objects, whether they are perfectly or imperfectly shaped. The candidates are chosen on the basis as a local maximum in the parameter space. The algorithm was applied to detect craters from the online available Planetary Science Archive Images of the Mars [12]. We obtained some convincing results in terms of crater detection.

The rest of the paper has been organized as follows. Section 2 discusses algorithmic steps. Section 3 presents sundry experimental results followed by some of our observations and a few clues for further investigation. Section 4 makes a conclusion.

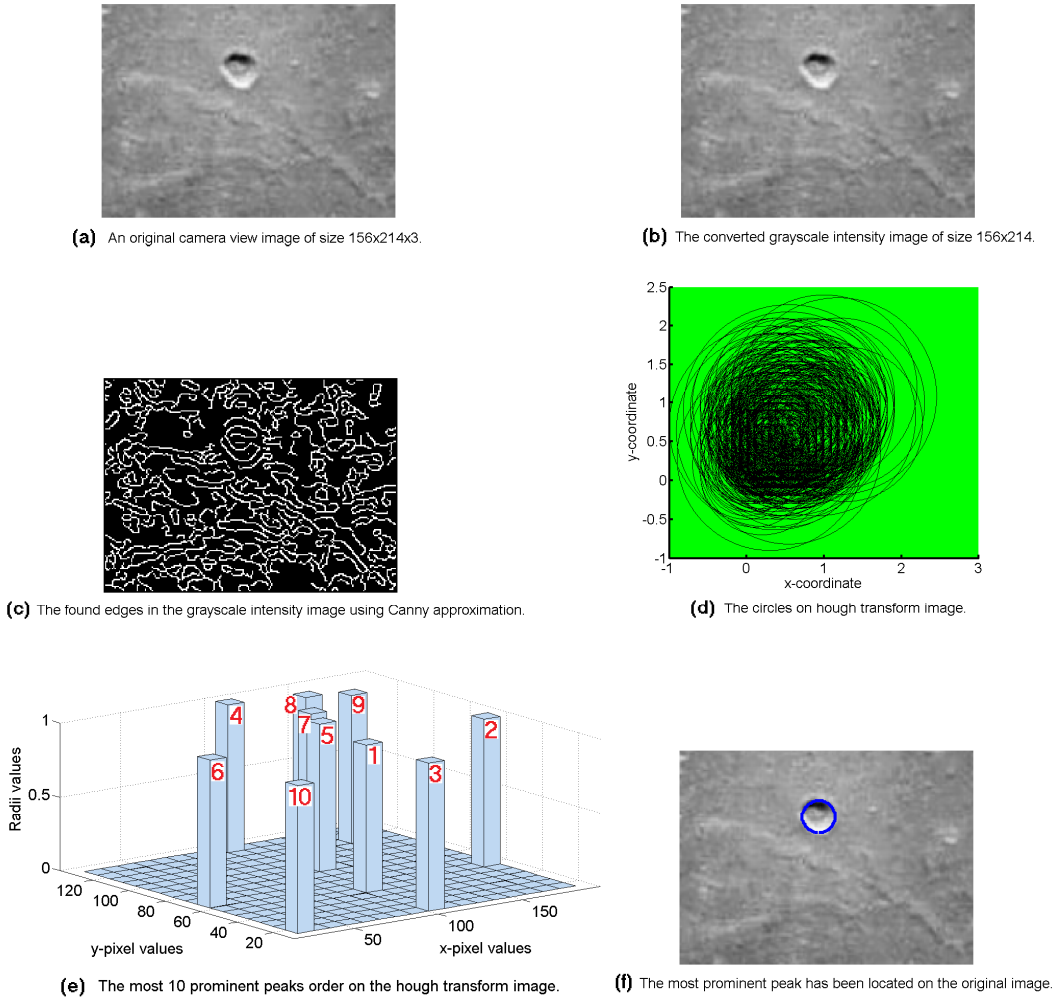

Figure 2. An example of the algorithmic steps of our implementation.

2. ALGORITHM

We have implemented a crater detection algorithm to detect craters from images of celestial bodies. Our algorithm is based on circular Hough transformation. The Hough transform is a technique which can be used to identify the parameters of a curve which best fits a set of given edge points. This edge description is commonly got from either a Roberts cross operator or a Sobel filter or a Canny edge detector. But these edge detectors may be noisy because there would be multiple edge fragments corresponding to a single whole feature. The output of an edge detector only determines the location of features an image, and then Hough transform determines both type of features and how many of them exist in the image. However, these properties of Hough transform provide us a reasonable selection for crater detection without limiting the possibilities to one astronomical object. It constructs candidate objects that resemble the looked-for objects, whether they are perfectly or imperfectly shaped. The candidates are chosen on the basis as a local maximum in the parameter space. Standard Hough transform and circular Hough transform are used in many computer vision applications. The standard Hough transform uses the parametric representation of a line to detect straight line. The input of this transform is usually a binary image containing the edge pixels. During the transform, it iterates through the edge points and calculate all {angle, distance} pairs for them. Each sinusoid curve belongs to a point. The crossing of two sinusoids indicates that the two corresponding points belong to the same line. The more sinusoids cross a given point, the more edge points are on the same line. However, we have implemented the circular Hough transform to detect astronomical objects such as craters. The circular Hough transform relies on equations for circles. Thus it has 3 parameters namely the radius of the circle as well as the x and y coordinates of the center. A larger computation time and memory for storage are required to compute these parameters. Thus it increases the complexity of extracting information from an image. For this reason, the radius of the circle may be fixed at a constant value. For each edge point, a circle can be drawn with that point as origin and radius. The circular Hough transform also uses a 3D array with the first two dimensions indicate the coordinates of the circle and the last third specifying the radius. The values in the array are increased every time a circle is drawn with the desired radius over every edge point. The array, which kept counts of how many circles pass through coordinates of each edge point, proceeds to a vote to find the highest count. The coordinates of the center of the circles in the images are the coordinates with the highest count. Suppose that Figure 2 (a) demonstrates an image of the Moon surface. We are interested to look for specific patterns which exist on its surface. Especially, there exists a visual crater in it. How can we detect that? The images of Figure 2 (b)-(f) depict the algorithmic steps of our implementation to detect the crater.

3. EXPERIMENTAL RESULTS

3.1. Experimental setup

Basically, we have performed our experiment on a computer of 8-Core CPUs at 3.50 GHz with 16 GB RAM. The algorithm was tested against the online available Planetary Science Archive Images of the Mars [12].

3.2. Detection results

The camera view images in Figure 3 (a), (c), and (e) depict three of the Planetary Science Archive Images of the Mars [12]. The algorithm had almost consistent results with satisfying accuracy as shown in the images of Figure 3 (b), (d), and (f), respectively. Although an excellent outcome of the algorithm is desirable for any application related to astronomy and astrophysics, the existing outcome of the algorithm is not so bad. But it is very important to try making improvements in

the field of computer vision which by extension makes advance in astronomy dynamically. Any observation made on the aspects, ideas, theories, and facts achieved through the analysis of data and astronomical imagery is worth partaking by considering as different outlooks and minds reach their aim in various ways. The observation can lead into more interesting connections made between computer vision and the entire field of astronomy. Without the help of computer vision algorithms, the factual data reached through the inputs of multiple sources the progress would have slowed down to somewhat of a standstill.

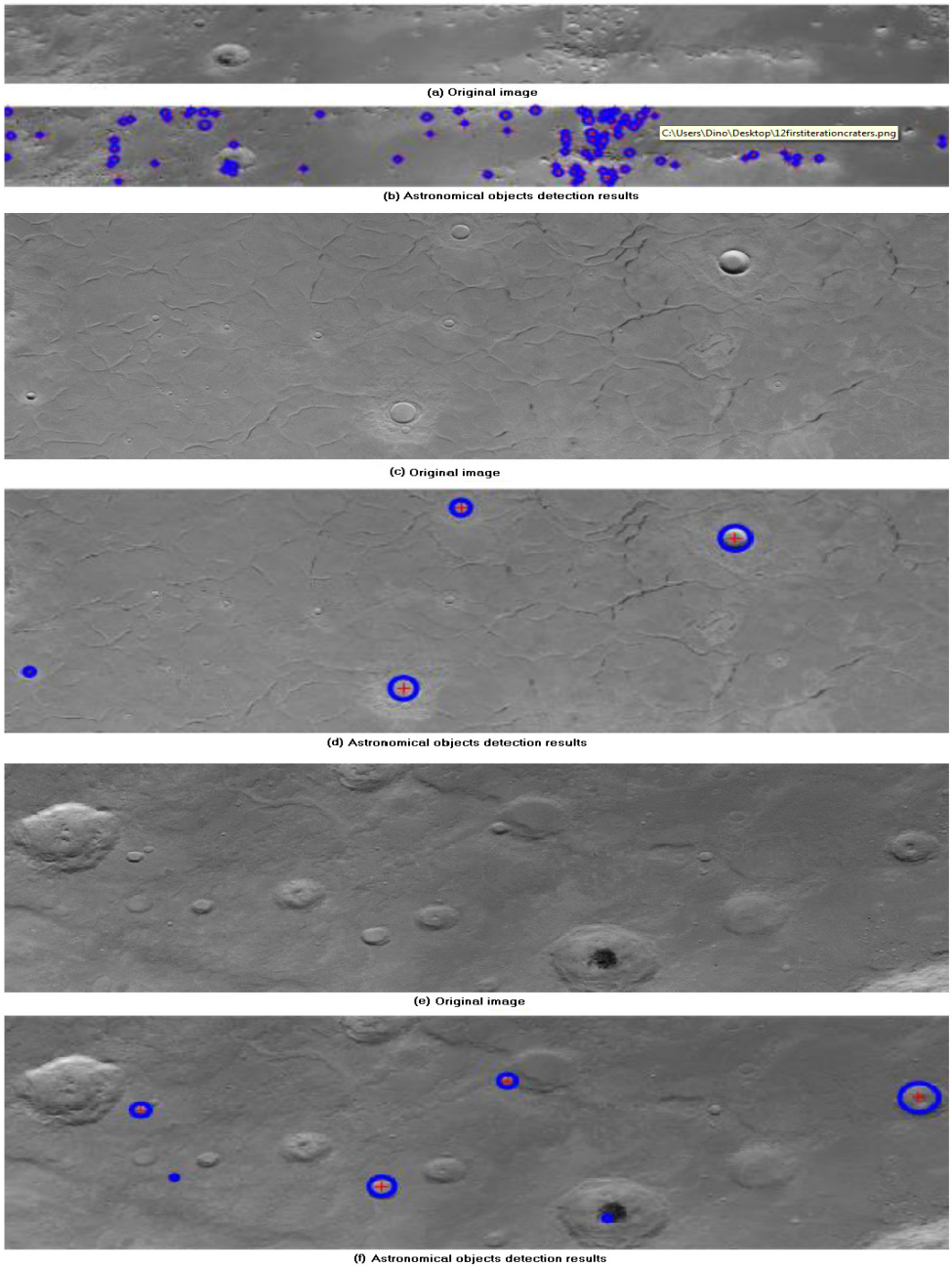

Figure 3. (a), (c), and (e) belong to camera view images; whereas (b), (d), and (f) depict the detected craters as pointed to the blue solid circles with red marked centers.

3.3. Our observations

As this paper has structural points, there is a way to gradually define the technical observations that will propel the idea further and inevitable lead to palpable success. It is a fair assumption to make that many of the aspects that surfaced as parts of the research might be unknown to a substantial percentage of potential readers which would place higher education as part of computer vision as an immediate success of this paper. Valuable findings will be resolved with a discourse on befitting areas and observations that always convey progress in development. When explaining spectro-polarimetric characterization of exoplanetary atmospheres [7] it was formulated and defined what the goal of that direction was. One of the findings was the understanding and recognition that the task of probing atmospheric composition and structure would be able to be completed using direct observing instruments. It is fascinating indeed. It was concluded that detecting these features would have requirements which might have to be met and that it could have obstacles in the form of errors which may have to be overcome. Once feasibility is evaluated, the action creates results. Another observation is that after going through a set of defined aspects in the realm of solar behavioral patterns, there are ways to make the detection of certain events much more efficient. Emphatically, it would take up fewer resources. In this case, SVMs created the improved situation during supernovae recognition.

Once the realization was made that anything which predicts or detects patterns in any analytical way can be applied to more than just what it was originally used, i.e., the doors opened to a much wider field of view. So far the focus was on comparing large areas that can be interchanged to work in different environments and situations. But the fact is that any type of pattern recognition algorithms would yield dissimilar results. If there are established pattern models for muscles, any given algorithms might produce stimulating results when applied to a much larger scales, e.g., potential maps of exoplanetary surfaces. The databases which technically could have an endless amount of data are not managed to the smallest points. For this reason, the multi-temporal database is used. It can be considered an inspiration for astronomers to thrive towards creating an easily accessible data warehouse which would make the target learning process more powerful. Another technical observation is the fact that upon understanding the position and advancement made when discussing the Gliese 229 star system it is official proof that when it comes to scales of that size. A small part of information on one object can alter and complete missing data to encompass the more knowledgeable way of thinking. Detecting crater boundaries was one of the more palpable results. In the case of creating the resulting images, the findings were based on the different ways astronomical objects behave that are still susceptible to comparison and in that way comprehension too.

One can try to make improvements in the field of computer vision which by extension makes progress in astronomy and astrophysics in a dynamic way. It is worth mentioning that any observation made on the aspects, ideas, theories, and facts achieved through the analysis of data and astronomical imagery is worth dealing. Because of diverse views and minds reach their goal in diverse ways. Without the aid of computer vision algorithms the progress of the factual data reached through the inputs of multiple sources would have slowed down to somewhat of a standstill. Consequently, when focusing on establishing advancements the factors such as the possibility to identify exoplanets, categorize astronomical objects, and define the details in a high resolution image of a planet's surface with the help of computer sciences should be insisted. Branches of astronomy and astrophysics can be connected effortlessly without worrying about the apparent intense differences. Many research works connect to the astronomical object surface study in a productive way through the analysis of universal events e.g., supernovae and the structural categorization of exoplanets. This should drive any person with an interest in astronomy as well as computers to try and create the most effective applications using astronomical imagery. It can be observed that through any situation and by all means we can use

computer vision algorithms to find out more about any astronomical and astrophysical aspect. Many researches were facing towards a focal point of matter as target analysis. For analyzing a small sector of the observable universe, we can use computer vision algorithms to determine whether a black hole or absence of light exists there. The absence of light towards the center of a distant area can be categorized undoubtedly much more efficient with computer vision algorithms and their implementations. By some luck, if a method is invented to record a miscellaneous type of aspect of the Universe (e.g., dark energy), then the data gathering and analyzing method will clearly be through computer vision means.

3.4. Future works

As the inevitable research in the field of astronomy and astrophysics continues, there will be separate future works and projects. A web application would be developed to focus on assisting astronomers, astrophysicists, and inquisitive stargazers to acquire factual information on astronomical data. Such web application can eliminate all existing redundant steps. Many computer vision algorithms are used in astronomy and astrophysics. A dedicated astronomical library for the beginners with unique and essential features would be implemented. The presented solution of this paper would be implemented on a larger scale with a more functional duality.

4. CONCLUSION

We implemented a computer vision algorithm to detect craters in celestial bodies. The efficacy of the algorithm was satisfactory for many applications of astronomy and astrophysics. We also presented some observations connected among computer vision, astronomy, and astrophysics. Without any shadow of doubt, we can conclude that out of computer vision algorithms the advancement of astronomy and astrophysics would have slowed down to somewhat of a deadlock.

ACKNOWLEDGEMENT

The authors would like to thank Mr. Dino Sudžuković for his numerous presentations on the course of CS601 Advanced Computer Vision during the spring semester of the academic year 2016-2017 at International University of Sarajevo (IUS), Sarajevo, Bosnia and Herzegovina.

REFERENCES

[1] Takahashi, J., Matsuo, T., Itoh, Y.: Feasibility of spectro-polarimetric characterization of exoplanetary atmospheres with direct observing instruments. Astronomy & Astrophysics 599 (2017) A56.

[2] Bourrier, V., Ehrenreich, D., Wheatley, P., Bolmont, E., Gillon, M., de Wit, J., Burgasser, A., Jehin, E., Queloz, D., Triaud, A.: Reconnaissance of the TRAPPIST-1 exoplanet system in the Lyman-α line. Astronomy & Astrophysics 599 (2017) L3.

[3] Erkeling, G., Luesebrink, D., Hiesinger, H., Reiss, D., Jaumann, R.: The multitemporal database of high resolution stereo camera (hrsc) and planetary images of mars (muted): A tool to support the identification of surface changes. European Planetary Science Congress 10 (2015) 1–2.

[4] Romano, R.A., Aragon, C.R., Ding, C.: Supernova recognition using support vector machines. In: International Conference on Machine Learning and Applications (ICMLA), IEEE (2006) 77–82.

[5] Nagel, W., Mecke, J., Ohser, J., Weiss, V.: A tessellation model for crack patterns on surfaces. Image Analysis & Stereology 27(2) (2011) 73–78.

[6] Upadhyay, A., Ray, P.: Crater boundary detection and size frequency distribution (SFD) using MATLAB. Project Report 116, Indian Institute of Remote Sensing, Indian Space Research Organization, Bangalore, India (2011).

[7] Nakajima, T., Tsuji, T., Takeda, Y.: Physical properties of gliese 229b based on newly determined carbon and oxygen abundances of gliese 229a. The Astronomical Journal 150(2) (2015) 53.

[8] MSL: Mars Science Laboratory, Curiosity Rover, Multimedia, Raw Images (2017) https://mars.nasa.gov/msl/multimedia/raw.

[9] Honda, R., Konishi, O., Azuma, R., Yokogawa, H., Yamanaka, S., Iijima, Y.: Data mining system for planetary images-crater detection and categorization. In: Proceedings of the International Workshop on Machine Learning of Spatial Knowledge in conjunction with ICML, Stanford, CA. (2000) 103–108.

[10] Meng, D., Yunfeng, C., Qingxian, W.: Method of passive image based crater autonomous detection. Chinese Journal of Aeronautics 22(3) (2009) 301–306 2, 3 11. Mu, Y., Ding, W., Tao, D., Stepinski, T.F.: Biologically inspired model for crater detection. In: The 2011 International Joint Conference on Neural Networks. (July 2011) 2487–2494.

[12] PSA: Planetary Science Archive (2017) https://archives.esac.esa.int/psa/#! Table%20View.

AUTHOR INDEX